



Surface deformations of 24 January 2020 Sivrice (Elazığ)–Doğanyol (Malatya) earthquake ($M_w = 6.8$) along the Pütürge segment of the East Anatolian Fault Zone and its comparison with Turkey's 100-year-surface ruptures

Orhan Tatar¹ · Hasan Sözbilir^{2,3} · Fikret Koçbulut¹ · Erdin Bozkurt^{4,5} · Ercan Aksoy⁶ · Semih Eski³ · Bülent Özmen⁷ · Hüseyin Alan^{8,9} · Yüksel Metin¹⁰

Received: 31 July 2020 / Revised: 27 September 2020 / Accepted: 30 September 2020 / Published online: 27 October 2020
© Springer Nature Switzerland AG 2020

Abstract

On Friday, January 24, 2020 at 20.55:11 local time (17:55 UTC), an earthquake with a magnitude of $M_w = 6.8$ has occurred in Sivrice district of Elazığ (Eastern Turkey). Focal mechanism solution is consistent with pure left-lateral strike-slip faulting; the location of the epicenter and fault mechanism suggest deformation along the Pütürge segment of the East Anatolian Fault Zone. A 10-day fieldwork was carried out along the Pütürge segment to study surface deformation; the geometry of the surface rupture and other seismic geomorphological structures were mapped and studied in detail. The field data are also correlated with satellite images. This paper, therefore, presents classification of seismic geomorphological structures and discuss intimate relationship between fault geometry and stress field in the region. Seismic geomorphological deformation and related features of the Sivrice (Elazığ) earthquake are observed in the area between Gezin (Elazığ) and Ormaniçi (Pütürge) villages; they are classified into two as seismotectonic and seismo-gravitational features. Field observations confirm that seismo-gravitational structures develop along both Gezin–Sivrice–Doğanbağı and Doğanbağı–Çevrimtaş–İlincak–Koldere–Ormaniçi sections of the Pütürge segment, while surface rupture is mapped as seismotectonic structure only along the Doğanbağı–Çevrimtaş–İlincak–Koldere–Ormaniçi section. Small-scale landslides, rock falls, feather cracks along asphaltic roads, and laterally discontinues ground failure-related features are common seismo-gravitational structures that developed along the fault zone. In addition, small-scale lateral spreading and liquefaction structures are common especially in areas where fault-perpendicular streams meet the Karakaya Dam reservoir. The surface rupture is mapped as stepping and overlapping en échelon fractures along elongated pressure ridges between Çevrimtaş and Doğanbağ villages, to northwest of İlincak village, along 1.5-km-long pressure ridge between Topaluşağı and Doğanyol, across the elongated hill that developed on an alluvial fan to the northwest of Doğanyol and in the area between Koldere and Ormaniçi villages. Surface fractures deforming the pressure ridges are all aligned parallel to the long axes of the ridges and display reverse components that give rise to small-scale pop-up structures. Interferometric SAR (DInSAR) studies indicate a 10-cm uplift in the northwestern block of the fault and a 6-cm subsidence in the southeast block. The difference in vertical movements between two blocks of the fault is interpreted to suggest that at least 30-km-long section of the Pütürge segment in the area between southwest of Sivrice and Pütürge is broken during the main shock. Although the focal mechanism solution of the main shock gives pure left-lateral strike-slip faulting, there is no significant left-lateral displacement observed during the fieldwork. This can be explained by the following: (1) left-lateral strike-slip displacement was not able to reach the surface; (2) left-lateral torque movement of the fault around a vertical axis during the earthquake, (3) restraining bend nature of the Pütürge segment, or (4) the presence of Pütürge metamorphics along the fault strike. It is also important to note that along most part of the Pütürge segment where surface rupture is observed, talus, colluvial or alluvial fan sediments are exposed; unconsolidated and/or poorly consolidated nature of these sediments may also be counted as one of the main reason for not observing horizontal displacement on the surface. When we compare these surface deformations with the surface ruptures that occurred in the last 100 years in Turkey, we suggest that the formation of the surface deformations is variable depending on: (1) the fault type and the state of regional

stress, (2) the magnitude of the earthquake, (3) the duration time of the earthquake and (4) the geomorphologic feature of landscape in relation to the lithologic and structural features of the rock units along the active fault zone.

Keywords Sivrice (Elazığ)–Doğanyol (Malatya) earthquake · East Anatolian Fault Zone · Pütürge segment · Seismic geomorphology · Turkey’s 100-year-surface ruptures

1 Introduction

Most part of Turkey lies on the Anatolian Plate, which is being forced westwards as a natural response to the collision between the Arabian Plate and the Eurasian Plate. This westward movement is accommodated by two large strike-slip

fault zones, the west–east-trending right-lateral North Anatolian Fault Zone (NAFZ) in the north and the SW–NE-trending left-lateral East Anatolian Fault Zone (EAFZ) in the southeast. Movement along the two fault zones has been responsible for many large and damaging high-magnitude historical and instrumental earthquakes (Fig. 1). The most

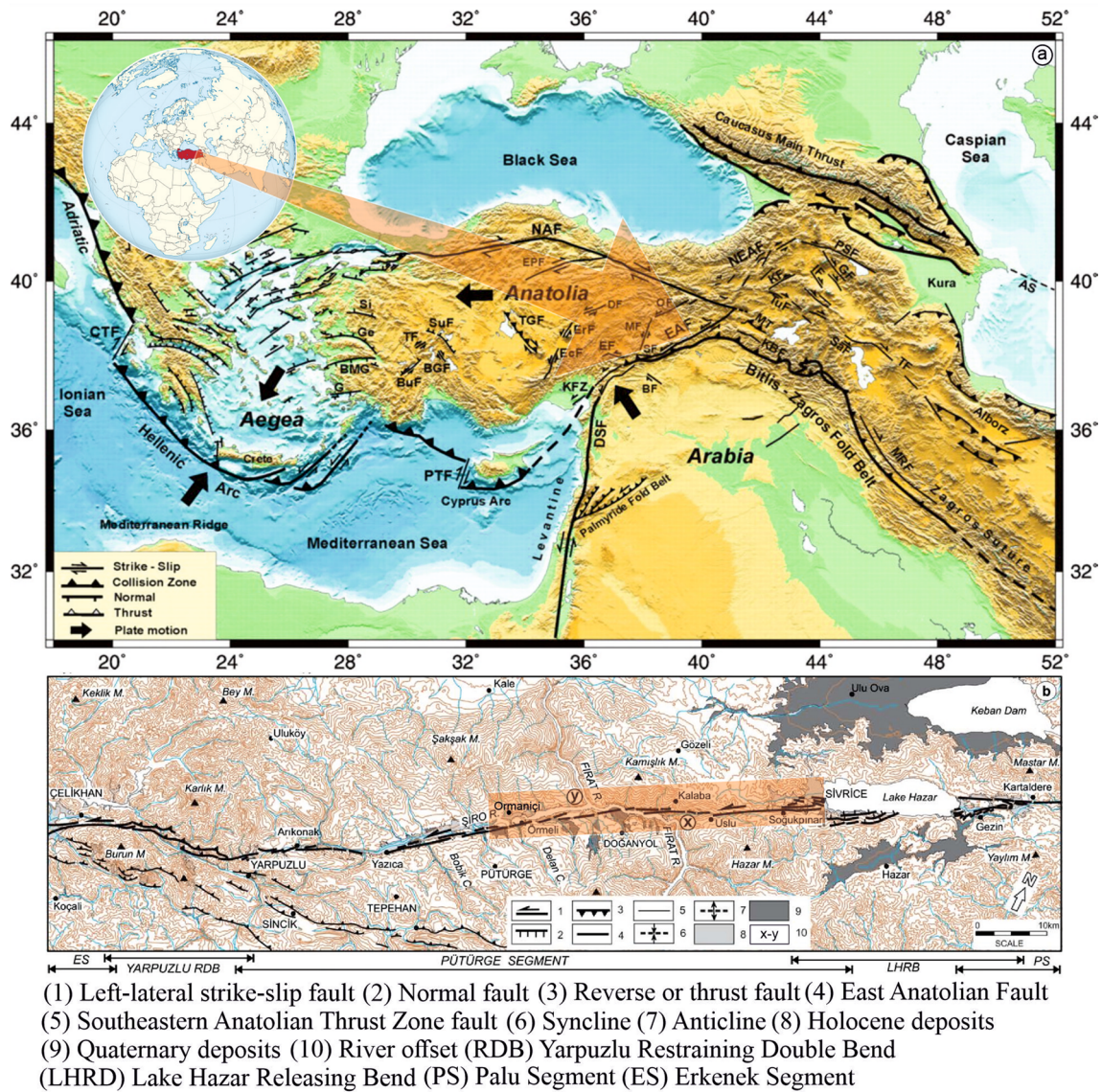


Fig. 1 a DEM map showing regional structural elements of Turkey and surroundings (Taymaz et al. 2007), b active fault map between Lake Hazar and Çelikhán (Duman and Emre 2013) showing the

shaded rectangle) the ruptured segment of East Anatolian Fault Zone. The faults are from Duman et al. (2012) and Emre et al. (2012)

recent strong earthquakes on the EAFZ prior to last devastating earthquake in 2020 are the May 1, 2003 Bingöl Earthquake (M: 6.4) and the March 8, 2010 Elazığ earthquake (M: 6.0).

At 20:55:11 local time (17:55 UTC) on the evening of Friday, 24 January 2020, an earthquake of magnitude $M_w = 6.8$ and a depth of about 8.06 km hit Elazığ province (eastern Turkey). The epicenter of the earthquake given by different centers falls to the northeast of Çevrimtaş near the village of Kalaba close to the town of Sivrice in Elazığ. The duration of the earthquake was reported as 20.4 s (AFAD). The earthquake was followed by numerous aftershocks, the strongest of which with a magnitude of 5.0 M_w . The focal mechanism, epicentral location and distribution of aftershocks are all consistent with the activity caused by movement along the main strand of the East Anatolian Fault Zone.

After the earthquake, field observations were made by many researchers in the region as brief note. Gökçeoğlu et al. (2020) stated that surface deformations are observed along the East Anatolian Fault Zone (DAFZ) on the alluvial deposits on the coast of Hazar Lake in Sivrice. According to these researchers, in addition to poor quality of structural materials, construction and workmanship, another important reason of severe damage to masonry buildings and infrastructure in Çevrimtaş and nearby villages is the observed surface rupture in the area.

According to the first findings, no significant and continuous surface rupture occurred in the earthquake area instead cracks, ground run-offs caused by vibration and gravity, and many landslides are common in some sections along the fault zone. It has been stated that not all earthquakes with this magnitude results in prominent and persistent surface rupture, and it can be explained by the authors with an aseismic creep occurring in shallow crust (İTÜ 2020). In the preliminary evaluation report by Boğaziçi University Kandilli Observatory and Earthquake Research Institute (KOERI 2020), the magnitude of the earthquake is $M_w = 6.5$ and the estimated length of surface rupture varies between 20 and 30 km, and that the earthquake is the result of movement along the Pütürge segment of the East Anatolian Fault Zone.

In a MTA report (Kürçer et al. 2020), surface deformation features (Riedel shear fractures, en-échélon tension cracks and surface fractures) are observed along approximately 48-km-long segment of the EAFZ in the area between Lake Hazar and Pütürge. The length of individual fracture, which continue in an en-échélon pattern, usually vary from a few meters to several hundred meters. No obvious lateral displacements are observed. Two paleoseismological trenches were also excavated on the surface rupture in Ilincakbaşı locality, 500 m south of Ilincak Village (Sivrice–Elazığ). Accordingly, at least three paleo-earthquakes are identified. These authors suggest, based on field observations and the distribution of January 24, 2020 earthquake aftershocks that

two sub-segments of the Pütürge segment were broken. They also claim that the earthquake source fault might be inclined to the northwest, because more damage occurred in areas northwest of the Pütürge segment, and the aftershocks are mostly concentrated on the northwestern block of the earthquake fault very close to the Pütürge segment. For the first time in this study, aligned gas degassing on the water surface of the Karakaya Dam Lake is recorded and photographed; the alignment is interpreted to locate the trace of surface rupture within the dam lake.

Despite the fact that there is considerable amount of preliminary reports available about the Sivrice (Elazığ)–Doğanyol (Malatya) earthquake, none presents a detailed account of earthquake-induced surface deformation features and discusses their significance. To fill this gap, we mapped and classified the seismo-gravitational and seismotectonic structures in the earthquake area, and compared them with the surface ruptures formed during the last hundred years in Turkey.

A summary of seismotectonic setting of the study area and seismogenic source of the earthquake will be given in the following section. Detailed description of mapped surface deformation features and their classification in relation to seismo-gravitational or seismotectonic behavior forms the subject of third section. After that, we focus on interferometric data for comparison with the field-based data. Finally, we present a table that summarizes information about earthquakes occurred on different active faults in Turkey during the last century. This table aims to explore if there is any relationship between earthquake magnitude, fault type, duration of the earthquake and formation surface rupture. Our results confirm the intimate relationship between earthquake magnitude, fault type and occurrence of surface rupture.

2 Seismotectonics

It is generally accepted that, in eastern Anatolia where the Sivrice (Elazığ)–Doğanyol (Malatya) earthquake occurred, the collision between Arabian and Eurasian plates took place at the end of Middle Miocene, and that late Miocene is the time of consequent contractional tectonics in the region (Şengör and Yılmaz 1981; Şengör et al. 1985; Yılmaz et al. 1993; Westaway and Arger 2001). The ca. N–S compressional deformation and consequent shortening has eventually resulted in the initiation of North Anatolian and East Anatolian transform fault zones (NAFZ and EAFZ, respectively); the associated ca. E–W extension has resulted in the formation of open fractures, many of which have served as pathways for volcanic activity in the region (cf. Yılmaz et al. 1987). The transform nature of the EAFZ was first recognized by Arpat and Şaroğlu (1972) and its importance for the regional seismicity and active tectonics during

Quaternary–Holocene time has been investigated by numerous researchers (McKenzie 1978; Arpat and Şaroğlu 1975; Dewey et al. 1986; Ambraseys 1988; Taymaz et al. 1991; Westaway and Arger 1996; Westaway 2003). The time of initiation of the EAFZ is proposed as Late Pliocene (Şaroğlu et al. 1987; Westaway and Arger 2001) or close to the latest Pliocene–Pleistocene boundary (Herece 2008).

2.1 The East Anatolian Fault Zone

The East Anatolian Fault Zone (EAFZ), which forms the seismic source of the Sivrice (Elazığ)–Doğanyol (Malatya) earthquake, is a major sinistral strike-slip fault zone in Turkey. It starts at the Karlıova triple junction, where the EAFZ meets the North Anatolian Fault Zone, in the northeast and runs southwestward for about 600 km through Bingöl, Palu, Hazar Lake, Pütürge, Sincik, Narlı, Türkoğlu regions and

extends up to the İskenderun Bay in the Mediterranean Sea area (e.g., Arpat and Şaroğlu 1972; Hempton and Dunne 1984; Aksoy et al. 2007; Emre et al. 2013; Khalifa et al. 2018) (Fig. 2a and b). The fault zone comprises several short left-lateral fault segments and associated strike-slip basins; Lake Hazar is one of those basins. Hazar Lake is a NE–SW-trending transtensional basin in the central parts of the EAFZ in the area between Sivrice to the SW and Gezin to the NE (Fig. 2b).

A detailed account of the fault geometry and segment structure of the East Anatolian Fault Zone, based on 1:25,000-scale re-mapping of active faults, available seismological and palaeoseismological data, is well documented in Duman and Emre (2013). The main fault runs as single main fault trace of a narrow deformation zone in the area between Karlıova and Çelikhan. To the west of Çelikhan, the fault branches off two strands as southern and northern;

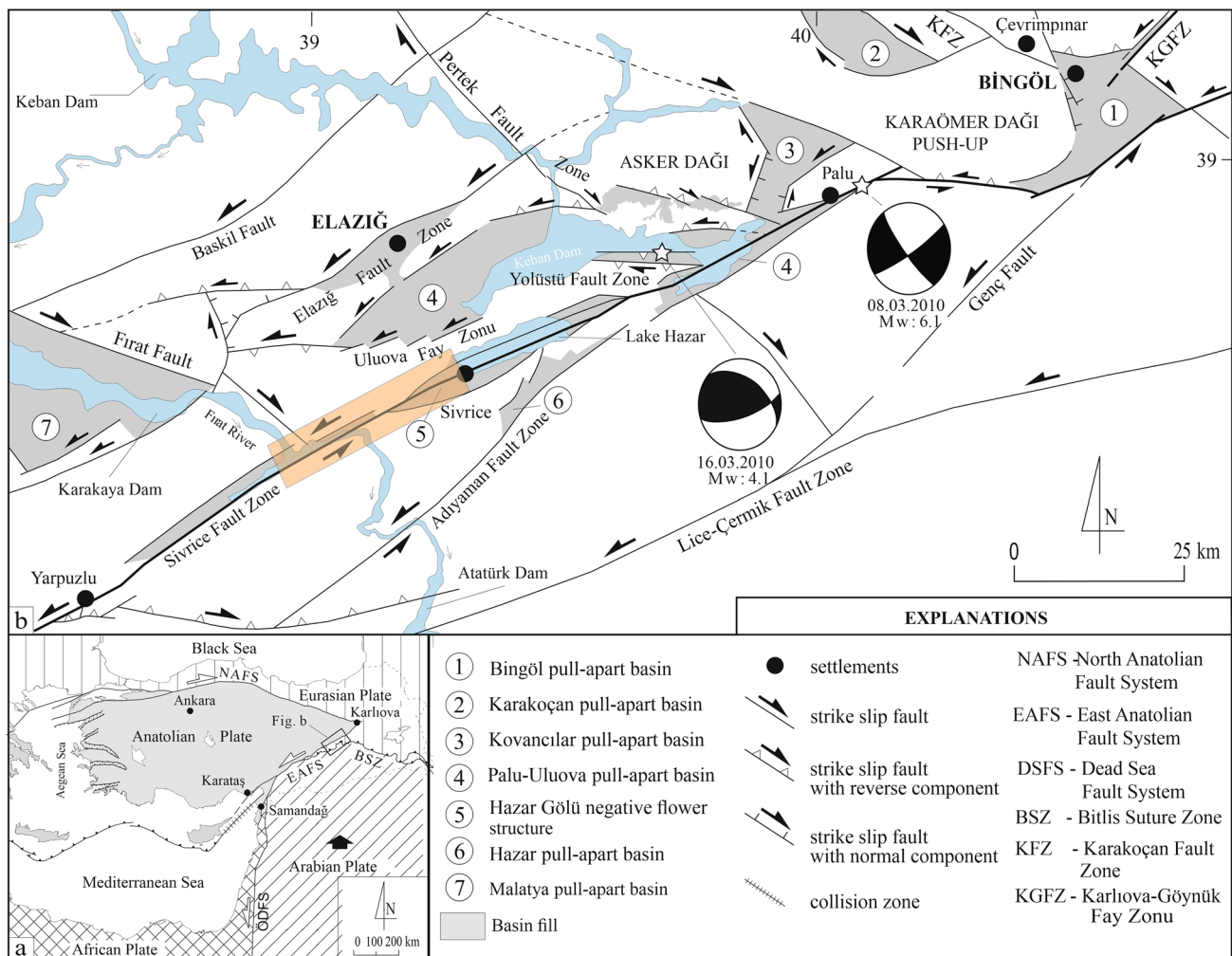


Fig. 2 a Simplified map showing major neotectonic structures of Turkey. EAFZ—East Anatolian Fault Zone; DAFZ—Dead Sea Fault Zone; NAFZ—North Anatolian Fault Zone. b Geological map of the

East Anatolian Fault Zone in the area between Yarpuzlu (Adıyaman) and Bingöl (modified from Koçyiğit et al. 2003; Çolak et al. 2012)

the latter is termed the Sürgü-Misis fault system. These strands are further divided, based on the stepovers, bends and abrupt changes in the general strike, into several fault segments with variable lengths and strikes. The main strand comprises, from northeast to southwest, Karlıova, Ilıca, Palu, Pütürge, Erkenek, Pazarcık and Amanos segments (see Fig. 2 in Duman and Emre 2013). Each segment comprises several sections as well. Several morphotectonic features confirm the Holocene activity of these segments.

The Palu segment occurs in the area between Palu and Gezin (Maden, Elazığ) districts to the northeast of the Lake Hazar, whereas the Pütürge segment is located in the area between southwestern margin of the Lake Hazar and Yarpuzlu district (Sincik, Adıyaman). Pütürge segment controls linear stream valleys in a mountainous terrain along most of its trace, where the faults cut into the basement rocks (Precambrian–Mesozoic Pütürge metamorphics, Cenonian Guleman–Kömürhan ophiolites and Eocene Maden Complex) (e.g., Hempton 1985; Herece and Akay 1992; Herece 2008; Duman and Emre 2013). The measured sinistral offset of the basement rocks and morphological features in the Fırat (Euphrates) River valley vary from 9 to 22 km (Arpat and Şaroğlu 1975; Hempton 1985; Herece and Akay 1992; Westaway and Arger 2001; Westaway 2003; Herece 2008; Çelik 2008; Duman and Emre 2013). Whereas the Fırat River valley itself is offset sinistrally by about 11 km along the Hazar-Şiro fault of the Pütürge segment (Duman and Emre 2013). Holocene fault scarps are common along the Pütürge segment; there is, however, no solid evidence about the formation of surface rupture as a result of latest seismic activity.

Left-lateral displacement along the EAFZ is also confirmed by seismological observations (Örgülü et al. 2003; Türkelli et al. 2003). Bulut et al. (2012) investigated the seismic activity along the EAFZ and fault kinematics based on recordings from a densified regional seismic network. The distribution of hypocenters suggests that the EAFZ is characterized by NE–SW and E–W oriented sub-segments that are sub-parallel to the overall trend of the fault zone. Faulting mechanisms are predominantly left-lateral strike-slip and thus in good correlation with the deformation pattern derived from regional GPS data.

During the instrumental period, the westward motion of Anatolian platelet along the NAFZ is about 2.5 cm/year, while it is about 1 cm/year along the EAFZ (Reilinger et al. 2006; Özener et al. 2010). The rate of motion along the EAFZ is variable between 4 and 10 mm/year. Westaway (2003) suggested for 4.0–4.6 mm/year which is consistent with GPS data reported in McClusky et al. (2000). Özener et al. (2010) argued for 10 mm/year, while Duman et al. (2017) proposed a rate of 7 mm/year for the Pütürge segment. In a more recent study, Aktuğ et al. (2016) collected and analyzed new survey-type GPS data, and

homogeneously combined published velocities from other studies, and this forms the most complete GPS data set covering the EAFZ. Their results show that while the slip rate of the EAFZ is nearly constant (~ 10 mm/year) to the North of Türkoğlu, it decreases to 4.5 mm/year in the south. The results also confirm two well-known seismic gaps across the EAFZ, Palu-Sincik and Çelikhhan-Türkoğlu segments. These segments have slip deficits of 1.5 m and 5.2 m and have the potential to produce earthquakes with magnitudes of M: 7.4 and M: 7.7, respectively.

2.2 Earthquake activity during historical and instrumental periods

The Eastern Anatolian Fault Zone (EAFZ) is interpreted as the source of a series of major destructive earthquakes especially during the nineteenth and twentieth centuries (Ambraseys 1988). In particular, the Pütürge segment was described as a seismic gap that can produce a near future destructive earthquake (Duman and Emre 2013). In this regard, Lake Hazar and its surroundings were considered as seismically highly active region. Statistical analysis of microseismic study reveal a daily average of five events with magnitudes less than 3.0 in the Lake Hazar area (Çetin et al. 2003). In addition to all, historical records and paleoseismological studies clearly show that earthquakes with magnitudes greater than 7.0 have occurred in this region (Ergin et al. 1967; Ambraseys 1988; Eyidoğan et al. 1991; Ambrassey and Finkel 1995; Ambrassey and Jackson 1998; Tan et al. 2008; Baştürk et al. 2017; Köküm and Özçelik 2020); the 1874, 1875 and 1971 events in the Lake Hazar, Palu and Bingöl are the most well-known earthquakes. In May 1874, $M_s = 7.1$ earthquake severely damaged the Lake Hazar and its immediate surroundings. There is also evidence for deformed (folded) river terraces along Şiro river valley (Aktimur and Oral 1981 in Duman and Emre 2013).

There are limited number of research on the paleoseismic activity of different segments of the Eastern Anatolian Fault Zone (Çetin et al. 2003; Karabacak et al. 2011). Most trenches are opened along the Palu, Pazarcık and Amanos segments (Çetin et al. 2003; Karabacak et al. 2011; Yönlü et al. 2017). Çetin et al. (2003) excavated two exploratory trenches on the two main strands (Gezin fault and Hazar fault) of the Palu-Lake Hazar segment; they also made detailed field observations. The authors interpreted the results of trenching to suggest that there are two major surface rupturing earthquakes: 1874 ($M_s = 7.1$) and 1875 ($M_s = 6.7$). Some claims that 1875 surface rupturing event (Ambraseys and Jackson 1998) has occurred along the Pütürge segment (Nalbant et al. 2002; Herece 2008). The historical earthquakes (Ambraseys and Jackson 1998) and results of the paleoseismologic study (Güneyli 2002; Çetin et al. 2003) are interpreted to suggest that 1875 event

occurred along Lake Hazar releasing bend. Accordingly, the recurrence interval of a major ($M > 7$) earthquakes along Palu segment is estimated as minimum 100 ± 35 and maximum 360 years (Çetin et al. 2003) or as 350–400 years (Duman and Emre 2013). Thus, the time elapsed since 1789 Palu earthquake is about 230 years.

The slip deficits on the Karlıova and Palu segments for the latest major earthquakes are estimated as 1.46 and 1.40 m, respectively (Duman and Emre 2013). These authors also argued for the lack of data about the recurrence interval for major earthquakes on the Pütürge segment. Considering the interpretation of Ambrasey (1988) that the 1905 (M 6.8) earthquake may have occurred on the Yarpuzlu bend at the western tip of the Pütürge segment, Duman and Emre (2013) considered the ca. 100-km-long Pütürge segment as one of several seismic gaps along the main strand of the EAFZ.

The May 22, 1971 Bingöl earthquake (M_s : 6.8) during instrumental period affected Bingöl and its immediate surroundings, and caused a great loss of life and property (Ambrasseys 1989; Ambrasseys and Jackson 1998). The records show that 81 earthquakes with magnitudes 4.0 or greater occurred in the region in the last 85 years. Three earthquakes with magnitudes 5.0 or greater have occurred in Sivrice district. Some of the other destructive earthquakes ($M = 5.0$ or greater) along different segments of the EAFZ include August 11, 2004, February 9, 2007, February 21, 2007, March 9, 2010 and June 23, 2011 events that affected Sivrice, Karakoçan and İçme districts (Kalafat et al. 2010, 2011; Tan et al. 2011). The June 13, 2003 (M : 5.6) and November 26, 2005 (M : 5.3) events caused considerable amount of damage in the region but fortunately there were no loss of life. More recent September 17, 2010 (M : 4.8), April 4, 2019 (M : 5.2) and December 27, 2019 (M : 5.0) earthquakes all occurred along the Pütürge segment. Thus, there is an apparent increase in the seismic activity along the Pütürge segment during last 17 years period.

The last one, a moderate size earthquake occurred at 20:55:11 local time (17:55 UTC) on Friday, January 24, 2020 in Sivrice (Elazığ) and Doğanyol (Malatya) area. Turkish Republic Ministry of Interior, The Disaster and Emergency Management Presidency of Turkey (AFAD) Earthquake Department announced magnitude of the earthquake 6.8 (M_w), focal depth as 8.06 km and epicenter as Çevrimtaş village (0.81 km south of Sivrice). According to Bogaziçi University Kandilli Observatory and Earthquake Research Institute (KOERI), the magnitude, focal depth and epicenter of the earthquake are M_I : 6.6 (M_w : 6.5), 5 km and Çevrimtaş village (Sivrice). On the other hand, these parameters are 6.7, 11 km and Kalaba village (11 km NNE of Doğanyol) according to USGS (Fig. 3).

It is here suggested, based on the data published by both national and international institutions and organizations, fault plane solutions, personal observations on surface

deformation structures that the 6.8 (M_w) magnitude Sivrice (Elâzığ)–Doğanyol (Malatya) earthquake occurred along the Pütürge segment of the EAFZ.

This earthquake once again showed that Turkey is located in a geography where destructive earthquakes have frequently occurred throughout history owing to its geological features. As a result of the earthquake, it was observed that the property damages in Elâzığ city center were concentrated in different neighborhoods of the city center; in addition to the demolished buildings in Mustafapaşa and Sürsürü neighborhoods, there were also heavy damage in Abdullahpaşa district. Outside Elâzığ city center, one building was destroyed in Gezin village located near the Lake Hazar. As you go to the south-southwest, especially in the villages of Kösebayır, Doğanbağı, Kalaba, Görgülü, Duygulu, Ilıncak, and Çevrimtaş in the Karakaya Dam Lake area close to the epicenter of the earthquake, there are losses of life and property due to the collapse or severe damage of the houses. These villages occur mainly on the river banks, the old alluvial fan deposits, landslides, and loose young (Plio–Quaternary) sediments within the fault zone (Fig. 4).

3 Surface deformations of Sivrice (Elazığ)–Doğanyol (Malatya) earthquake

Surface deformations developed during and immediately after the Sivrice (Elazığ)–Doğanyol (Malatya) earthquake were examined and mapped in detail along 30 km damage zone between Gezin village and Sivrice during the 10-day field studies between January 25, 2020 and February 3, 2020. Locations of surface deformations are indicated in Fig. 4. Most of the surface deformation features are interpreted to occur due to seismic shaking and gravity that developed during or just after the main shock. In addition to these, surface deformation originating from tectonic forces has also developed due to stress distribution along the Pütürge segment. Observed surface deformation features can be evaluated as seismic geomorphological indicators of the earthquake. Seismic geomorphology examines the changes and causes of this type of deformation that occur on and/or near the earth surface during or immediately after the main seismic shock (cf. Audemard and De Santis 1991; Dramis and Blumetti 2005). Recognition and mapping of these structures are very important in revealing a region's seismic risk analysis (Dramis and Blumetti 2005). In this study, the surface deformation features developed in relation to the Sivrice (Elâzığ)–Doğanyol (Malatya) earthquake were examined under two main classes: seismotectonic and seismo-gravitational. Seismotectonic surface deformation occurs in the form of surface fractures and cracks, ascending-collapsing and longitudinal ridges that develop due to tectonic stresses, while seismo-gravitational surface

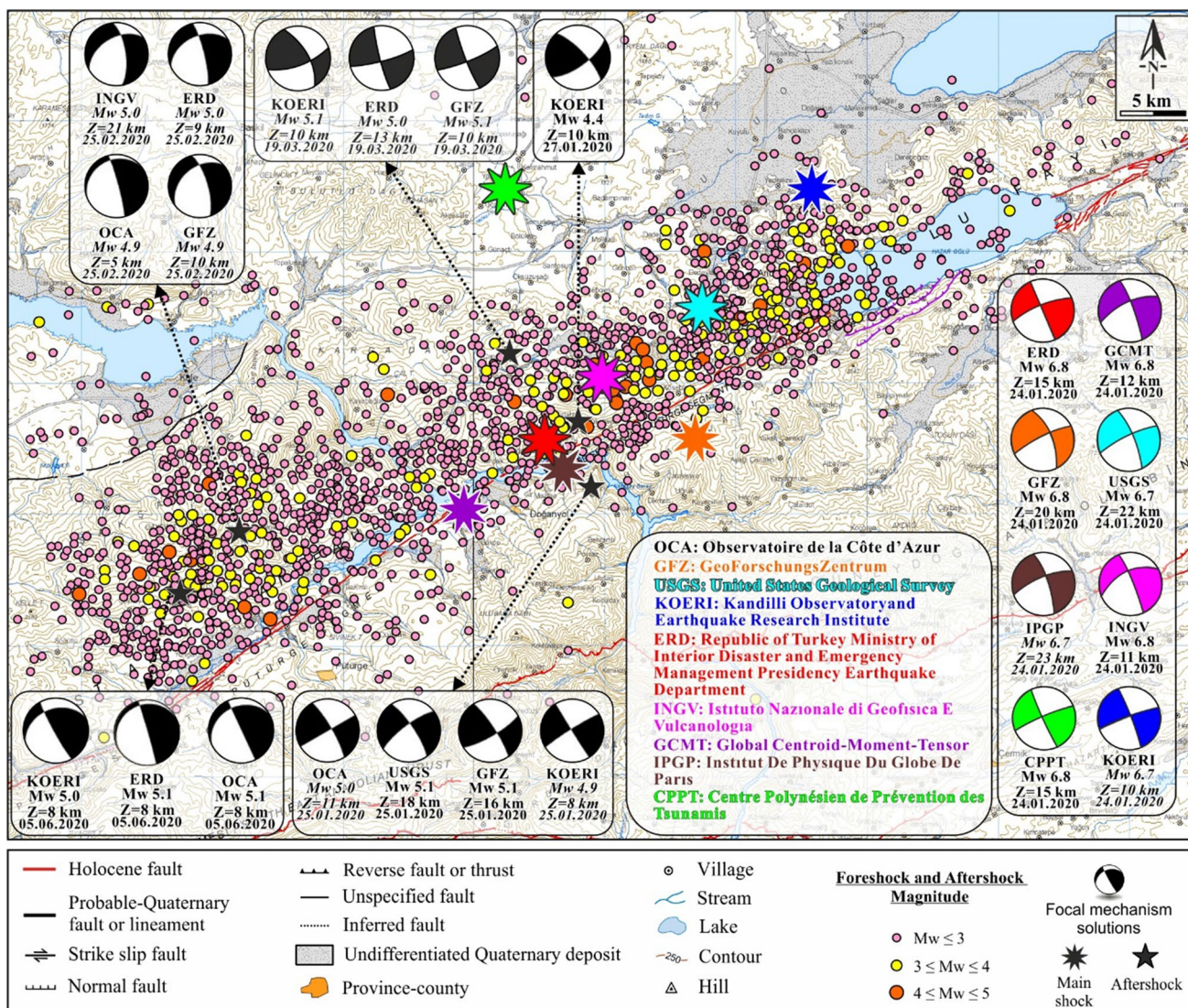


Fig. 3 A seismotectonic map showing the distribution of main and aftershocks of the 24.02.2020 Sivrice (Elazığ)–Doğanyol (Malatya) earthquake (Mw = 6.8). The active fault map is from Emre et al. (2011)

deformation features are in the form of mass movements, lateral spreading, capillary cracks and liquefaction (Table 1).

Field observations show that seismo-gravitational structures occur along the Gezin–Sivrice–Doğanbağı line, while both seismotectonic (as surface fracture and cracks) and seismo-gravitational structures are common on the Doğanbağı–Çevrimtaş–Koldere–Ormaniçi line to the southwest.

Surface deformation features occur along a ca. 30-km-long zone between Sivrice and Ormaniçi village and covers an area of up to 2 km in some places. This zone also forms the main part of the Pütürge segment. The 12-km left-lateral displacement of the Fırat River is also located within the central part of this deformation zone (Fig. 4).

A significant part of the surface deformation features developed in slope debris, colluvial materials and alluvial fans of Holocene age. Small-scale mass movements and capillary cracks have also been observed along the fault zone on road cuts and stabilized/asphalt roads. In places, fossil landslides were triggered in response to ground shaking and moved down slope under the influence of gravity; they appear as semi-circular sliding surfaces in the area.

3.1 Seismo-gravitational surface deformation

Among the seismo-gravitational structures that developed along/near the fault zone, include mass movements, such as small-scale landslides and rock falls, and capillary cracks observed along roads. Small-scale lateral spreading and

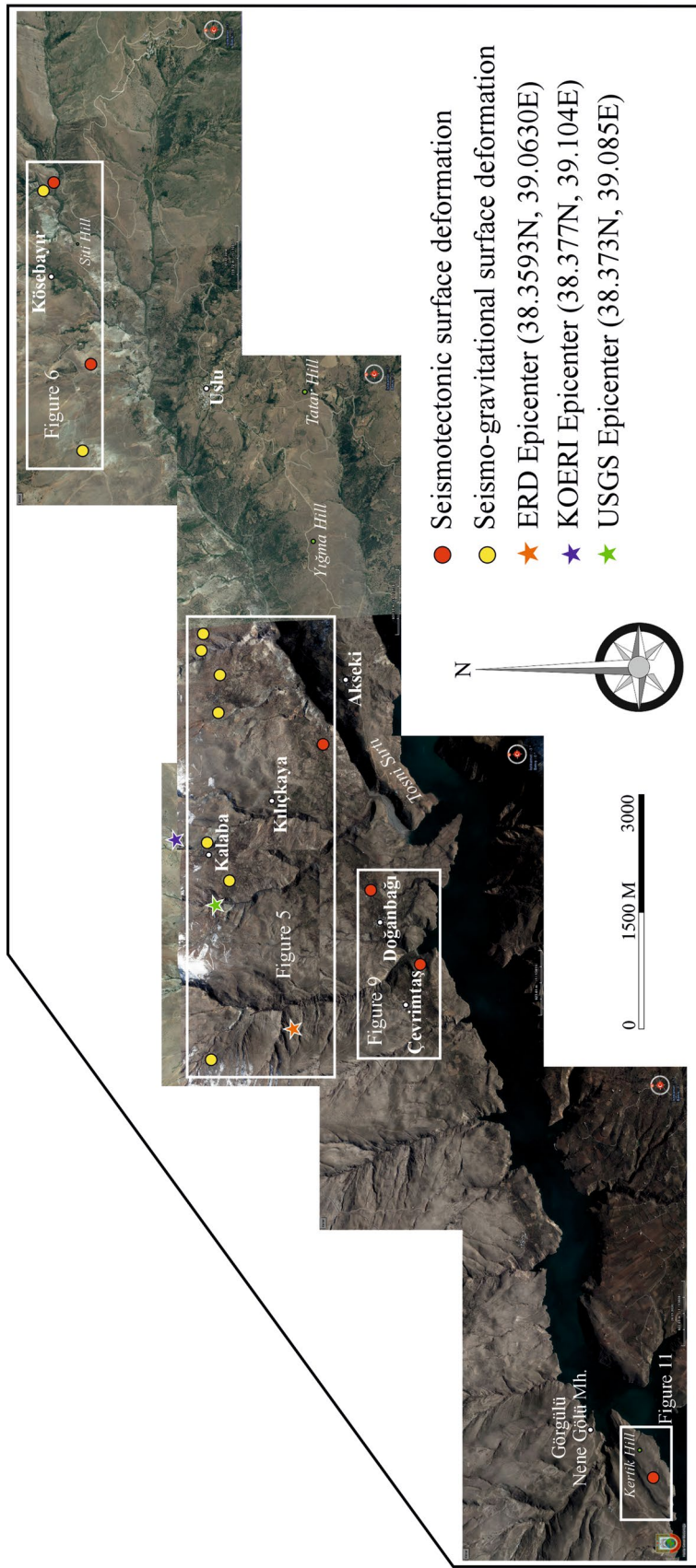


Fig. 4 HGM Küre map showing the location of surface deformation features that occurred in January 24, 2020 Sivrice (Elazığ)–Doğanyol (Malatya) earthquake. The red dots indicate the areas of the surface fracture, the yellow dots, areas where surface deformations are observed, and the blue, green and orange dots, the epicenter of the main shock given by KOERI, USGS and ERD, respectively

Table 1 Surface deformations developed in relation to the January 24, 2020 Sivrice (Elazığ)–Doğanyol (Malatya) earthquake

Seismotectonic surface deformation features (surface deformations developed due to tectonic stresses)
Uplift-collapse
Surface fracture and cracks
Elongated pressure ridge
Seismo-gravitational surface deformation features (surface deformations developed due to seismic shaking and gravitational force)
Mass movement
Liquefaction
Lateral spreading
Capillary cracks

liquefaction structures are also common, especially in the areas of alluvial fans (delta) where they form due to interaction between Karakaya Dam Lake and streams flowing perpendicular to the fault zone.

Detailed observations around villages of Kösebayır, Kılıçkaya, Doğanbağı, Çevrimtaş and Ilıncak located to the southwest of Sivrice district (Fig. 4) reveal that most deformational structures are seismo-gravitational in origin, and that dense network of capillary cracks are common structures along the road between Kösebayır and Kalaba villages.

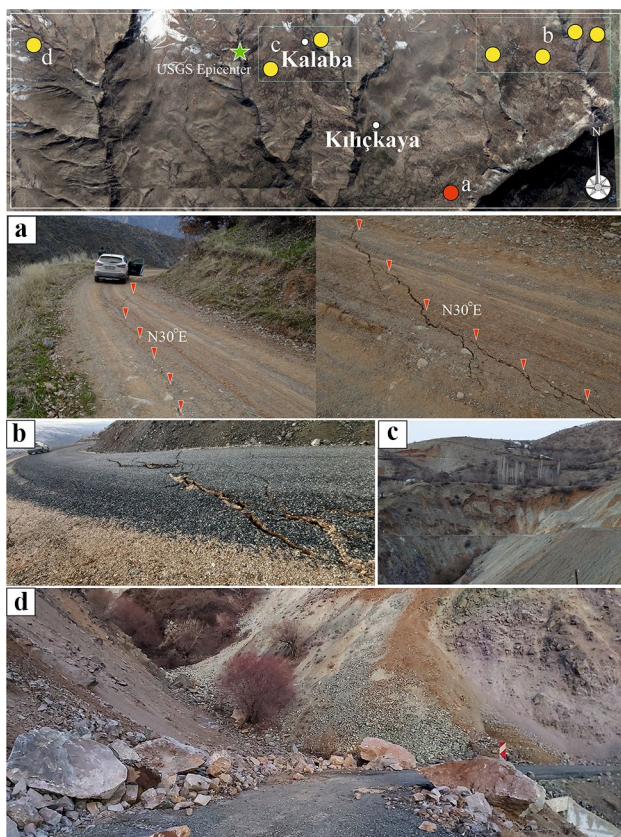


Fig. 5 a GoogleEarth image showing the location of seismo-gravitational landforms around Kalaba-Kılıçkaya villages. b–d Field views illustrating ground defeats and small-scale mass movements (e.g. rock fall)

Ground defeats up to 300 m in length developed in many sections along the road between Sivrice and Doğanbağı village. Such deformation features are particularly common on the east-southeast free slope of the road where vertical movements of up to 50 cm are observed. The ground defeats are mostly parallel to the slope direction but biased directions are also observed. These features caused the road to become unusable at many points (Figs. 5 and 6).

Lateral spreading and liquefaction structures are common in the alluvial fan-fan (delta) areas where streams flowing perpendicular to the deformation zone along the Doğanbağı–Çevrimtaş–Ilıncak line meet/interact the Karakaya Dam lake. Deformation of lateral spreading are represented by cracks normal and parallel to the fan axis, and display a step-like pattern towards the dam lake (Fig. 7). The slope debris and colluvial wedge materials stably located along high slopes were mobilized to form small-scale mass movements by sliding down the slope during shaking. Surface deformation features caused by this kind of seismo-gravitation are common especially on the slopes of Karakaya Dam Lake where the Fırat River valley is cut and displaced sinistrally by about 11 km along the Pütürge segment of the East Anatolian Fault Zone. These features suggest that materials, which are in critical balance on high slope, slid down and flowed during or immediately after the earthquake and caused the dam lake to narrow at certain rates (Fig. 7).

Detailed studies on the GoogleEarth and HGM Küre images taken at different times, it is understood that a number of fossil landslides became active during or after seismic shaking (Fig. 8a, b, red arrows). A surface fracture crack, which can be traced at short intervals along the ridge axis to the south of the mass movements, was observed (see red arrows in Fig. 8d). Vertical and steep capillary cracks developed on some parts of Sivrice–Doğanbağı road. These cracks pinch out laterally and show no vertical and horizontal movement but occur as open fractures with apertures ranging between 1 and 5 cm.

3.2 Seismotectonic surface deformation

Seismotectonic surface deformation features are observed in the form of surface fractures and cracks,

Fig. 6 **a** Google Earth image showing the location of seismo-gravitational landforms around Kösebayır village. **b–d** Field views illustrating ground defeats, such as capillary cracks and small-scale mass movements with down-slope surface deformation

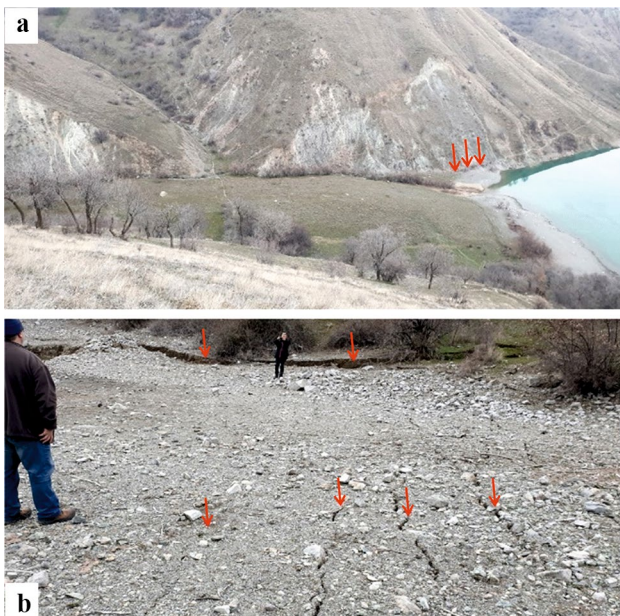
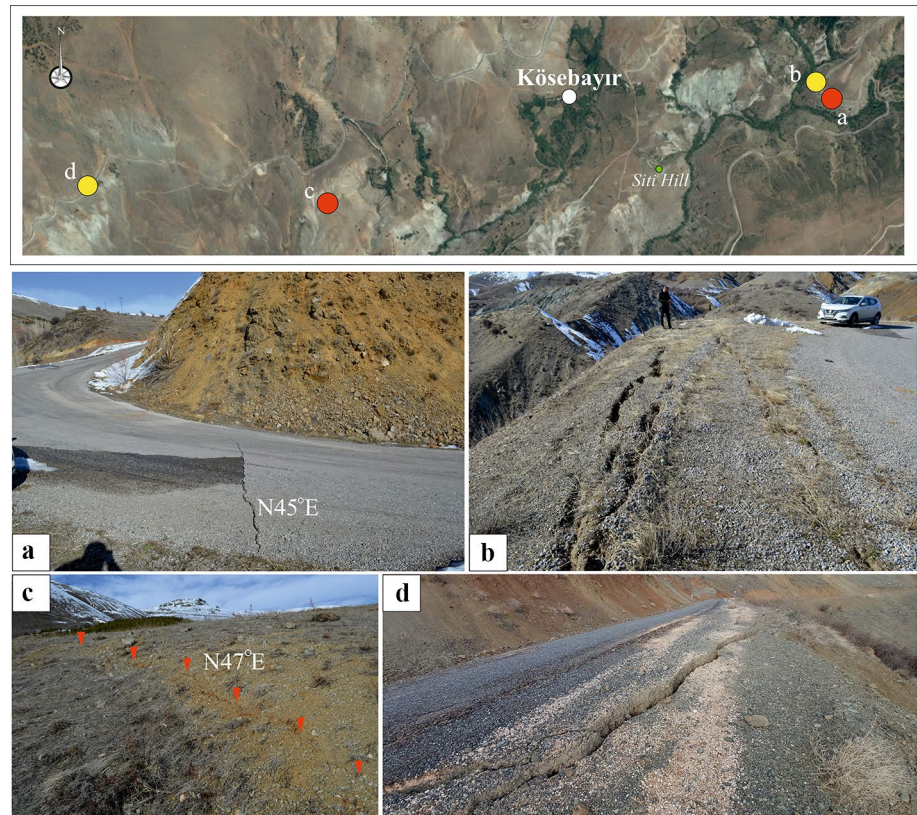


Fig. 7 **a** Seismo-gravitational surface deformation features that developed along the roads between Sivrice and Doğanbağı village; **b** lateral spreading structures formed in the alluvial fan deposits between Doğanbağı and Çevrimtaş villages

ascending-collapsing and longitudinal pressure ridges that develop due to tectonic stress. The locations of observed

seismotectonic surface deformations are given in Table 2. These features are observed along a pressure ridge between Çevrimtaş and Doğanbağı villages, and a 1.5-km-long pressure ridge that extends between Topaluşağı and Doğanlı to the northwest of Ilıncak; they commonly occur as surface fractures and cracks. Similarly, en-échélon fractures are observed along a pressure ridge around Koldere and Ormaniçi villages.

Surface cracks are aligned parallel to the slope of the pressure ridges and define pop-up structures. These structures are compatible with the restraining bend/overlap geometry tracked throughout the Pütürge segment. The surface cracks observed between Çevrimtaş and Doğanbağı can be traced for about 500 m along the axis of the NE–SW-trending ridge. There is no observable horizontal displacement along these the surface cracks. They rather show vertical displacements on both sides of the ridges and define pressure ridges resembling a positive flower structures (Fig. 9).

Çevrimtaş is one of the villages that have been damaged by the earthquake; it consists of two separate neighbourhood, while the upper neighborhood is located on the metamorphic rocks of the Pütürge Massif, the lower neighborhood is built right on the surface fracture of the Pütürge segment. The field observations confirm that most of the houses in lower settlement were severely damaged and collapsed, while there was loss of life as well. Personal communication with the villagers confirm that the ruins on the

Fig. 8 **a, b** Field views from the undurable materials moving down slope towards Karakaya Dam Lake during seismic shaking in the east of Ilıncak village, **c** GoogleEarth image and **d** HGM KÜRE orthophoto show that the fossil landslides on the dam lake slopes were reactivated during Sivrice (Elazığ)–Doğanyol (Malatya) earthquake

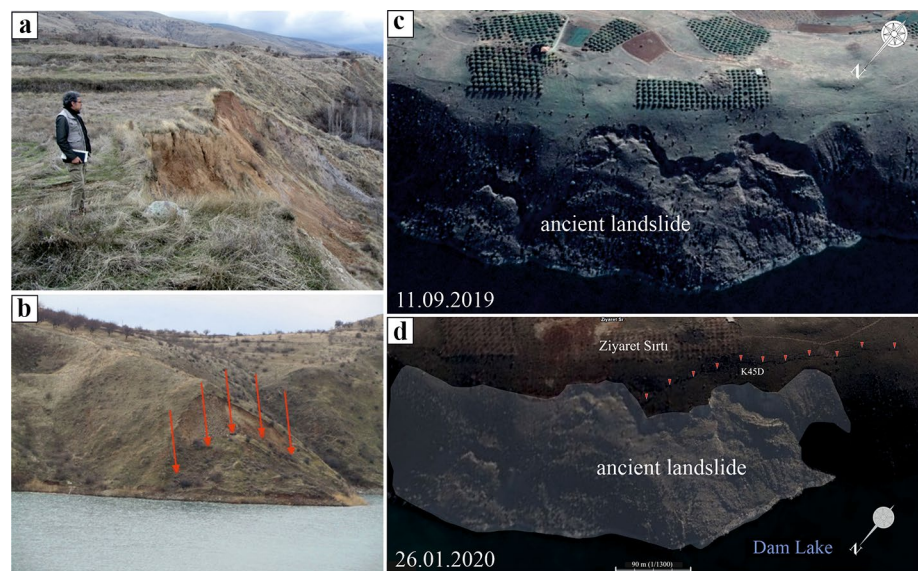


Table 2 Locations of seismotectonic surface deformation features (see Figs. 5, 6, 9, 11, 12, 13, 14 and 15 for location)

	Locality	Coordinates (Latitude–Longitude/WG84)	Lateral/vertical motion (cm)	Strike	Figure number in the text
1	SE Kılıçkaya	38.358755° 39.106496°	–	N 30° E	Figure 5, red dot on map
2	E Kösebayır	38.383613° 39.182535°	–	N 45° E	Figure 6a
3	SW Kösebayır	38.380418° 39.159696°	–/10	N 47° E	Figure 6c
4	SE Doğanbağı	38.352199° 39.081432°	–/5	N 50° E	Figure 9a
5	E Aşağı Çevrimtaş	38.349295° 39.069417°	–/10–40	N 40°–60° E	Figure 9b
6	Kertik Hill, SW Ilıncak	39.069417° 38.985810°	–/5–20	N 45°–50° E	Figure 11b–e
7	SW Ormaniçi	38.21155° 38.77415°	–/15–40	N 20°–60° E	Figures 12, 13 and 14
8	SW Ormaniçi	38.211354° 38.774332°	–/5	N 60°–80° E	Figure 15a–c
9	SW Ormaniçi	38.211820° 38.775003°	–	N 65° E	Figure 15d

ridge to the northeast of lower neighbourhood belong to the previous residential area of the village, and that it was destroyed by the earthquake in 1875. Local have then moved the village to the new location to southwest tip of the same ridge. It was observed that the surface fracture formed in the last earthquake also pass through the old settlement area (Fig. 10).

To the 4.5 km northwest of Doğanyol where 1.7-km-long NE–SW-trending elongated pressure ridge occurs. There, several surface cracks are developed during the earthquake. These deformation features are observed along the Kertik Tepe as right-stepping surface cracks and laterally discontinuous small-scale surface ruptures with reverse-slip component (Fig. 11).

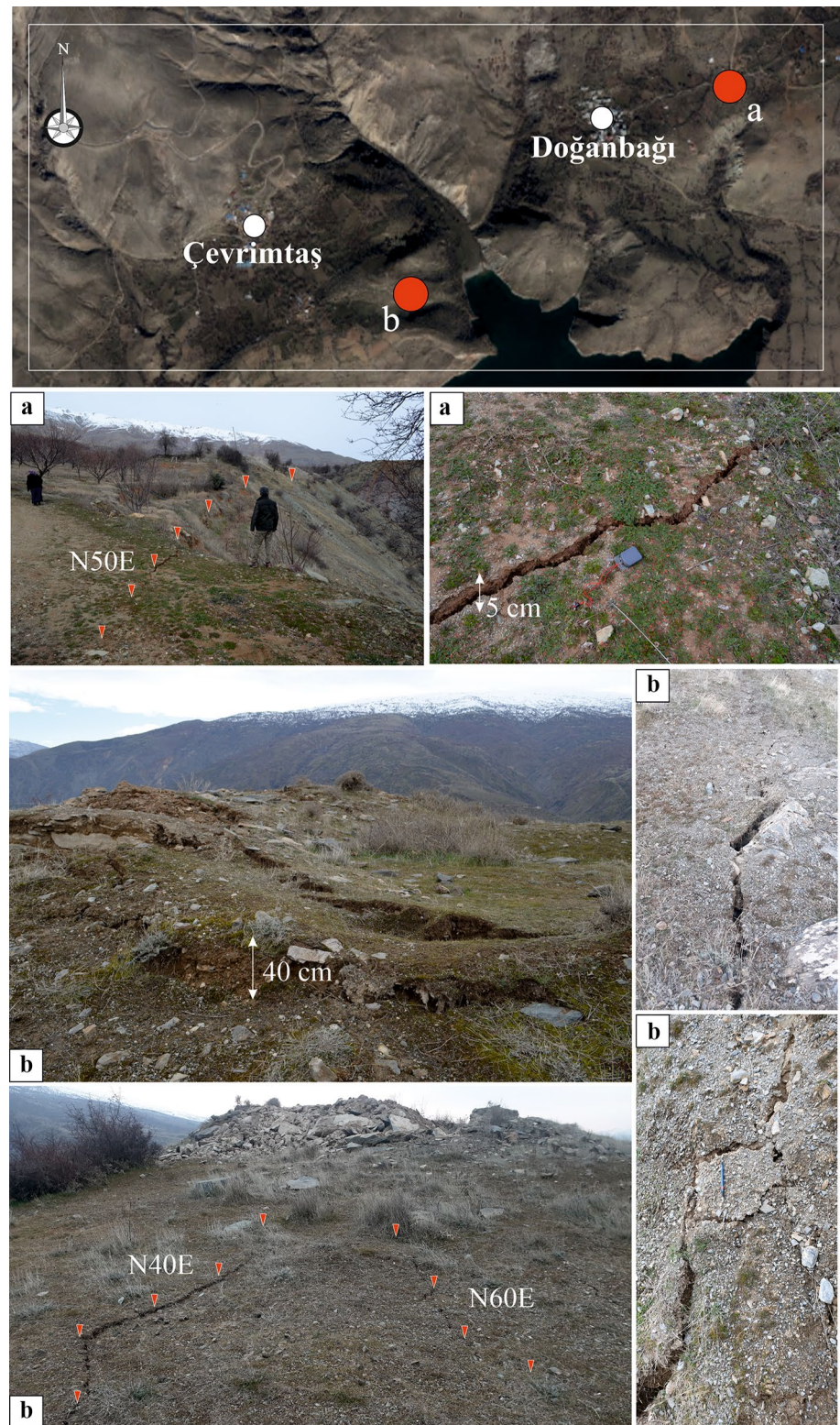
Surface deformation features are mapped in the south-east of Ormaniçi district in a N50°–60° E-trending zone of up to 500 m in length and 30 m in width (Figs. 12, 13, 14 and 15). Here, there are intermittent distances between individual fractures. The fracture network (Fig. 12a) and normal

vertical displacements along individual fractures are consistent with a typical sinistral strike-slip deformation.

4 Radar interferometry data

The Sentinel-1 (S-1) mission is based on a constellation of identical C-band synthetic aperture radar (SAR) satellites, which are currently comprised of the A and B units, to provide data continuity to European Space Agency's (ESA) (Yague-Martinez et al. 2016). The Sentinel-1 mission requirements ask for data products with different image characteristics and require implementation of four different measurement modes: Stripmap Mode, Interferometric Wideswath Mode, Extra-Wideswath Mode, and Wave Mode. The interferometric wide swath mode (IW) is a widely used in most applications as is done during this research. The Interferometric Wideswath mode will allow combining a large swath width (250 km) with a moderate geometric

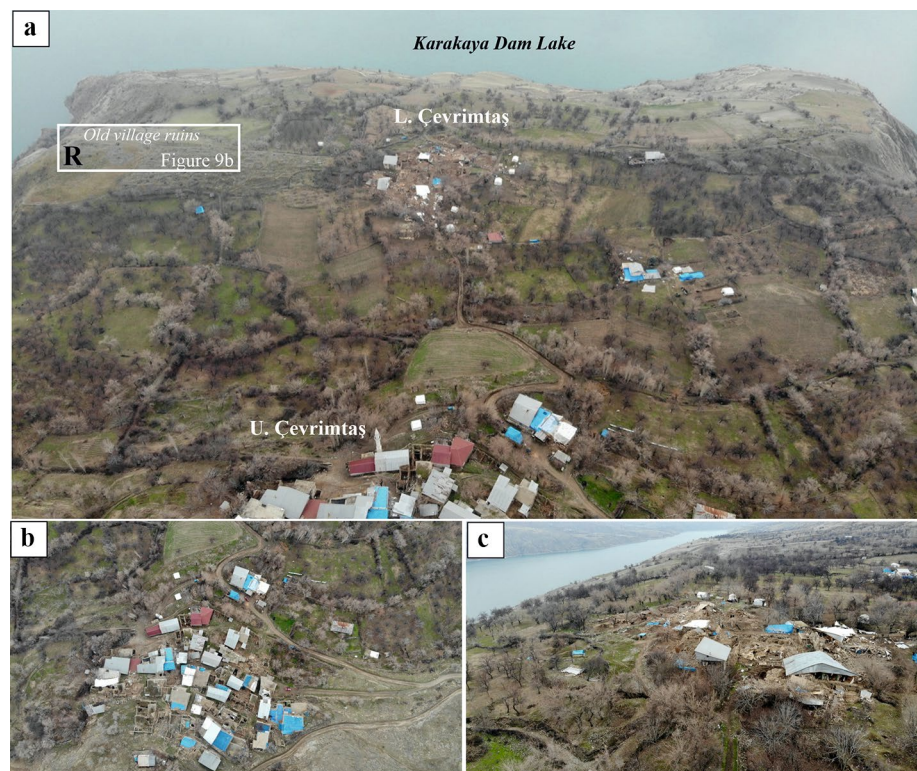
Fig. 9 GoogleEarth image showing the location of surface cracks around Doğanbağı (a) and Çevrimtaş (b). Field views showing surface rupture/cracks. Note the right-stepping capillary fractures in photo right b



resolution (5×20 m) (Torres et al. 2012). Detecting changes in the position of the Earth's surface requires two radar images of a selected area taken from approximately the same position at different times. Interferometry is based on

processing the pair of images to map out the differences in the reflected signals over the area. Differential interferometric synthetic aperture radar (DInSAR) can detect small differences in the distance between its position and the ground

Fig. 10 Field view from unmanned aerial vehicle (UAV) **a** showing the surface fracture passing through the east-south-east of the Çevrimtaş village. Note the extension of the fracture from the old village ruins (R) to the lower neighbourhood (Aşağı Çevrimtaş) and **b**, **c** from the upper neighborhood and lower neighborhood areas. Pay attention to the abundance of houses damaged in the lower neighborhood which is located on the surface deformation zone



as the land surface moves—whether up, down, or sideways. Especially, InSAR allows to see unrecognized faults or other potentially seismogenic subsurface structures and to better define the subsurface position of known structures (Helz 2005). DInSAR technique is based on the combination of two synthetic aperture radar (SAR) images acquired for the same area at different times from slightly different positions. The result of this combination is a new image known as interferogram, whose main phase component, after corrections for topography and earth curvature, is the ground displacement along the radar Line of Sight (LOS) (Sarychikhina and Glowacka 2015).

Previous studies demonstrated the promising capability of Interferometric SAR (DInSAR) techniques for studying co-seismic deformation. Interferometric analysis using the Sentinel-1's SAR dataset is one of the effective methods available to detect tectonic displacements associated with East Anatolian Fault Zone (EAFZ) in the January 24, 2020 Sivrice (Elazığ)—Doğanyol (Malatya) earthquake. For generating interferogram, minimum two S-1 data are required. One image is used for the master and others is the slaves (usually the new ones). The phase of SAR data represents the phase difference between the two images; the amplitude of both SARs images is multiplied. In this study, we generated co-seismic interferogram from S-1 IW data using images acquired from descending orbit (Table 3). We constructed phase and deformations images using SNAP software distributed by ESA (2020). The first step corregistration ensures

that each ground target contributes to the same (range, azimuth) pixel in both the master and the slave image. Others steps are interferogram generation for removing the flat-Earth phase, deburst to merge the results of the processing from all subswaths, topographic phase removal for simulate an interferogram based on a reference DEM and subtract it from the processed interferogram, Goldstein phase filtering for reducing noise (Goldstein and Werner 1998). Another important processing step is phase unwrapping, which is necessary for displacement maps. After these steps are completed, we obtained phase interferogram and displacement maps.

The January 24, 2020 Sivrice (Elazığ)—Doğanyol (Malatya) earthquake represents the largest seismic event affecting surface ever observed with modern DInSAR techniques. Co-seismic measurements allow us to estimate vertical displacement and to prepare a deformation maps (Fig. 16). Surface deformation after the earthquake is visible in the phase map (Fig. 16a) and we find mean 10 cm uplift on NW block and maximum—6 cm subsidence on SE block (Fig. 16b). The line, which is clearly evident between the subsidence and uplift block, corresponds to the area where the surface rupture may form. The 30-km-long surface rupture starts from the SW of Sivrice and continues along the Fırat River, ends between the Pütürge and the Doğanyol (Fig. 16b). The distribution of surface deformation features, such as landslides, tension cracks, etc. caused by aftershocks, occur in a zone that reaches to length of about

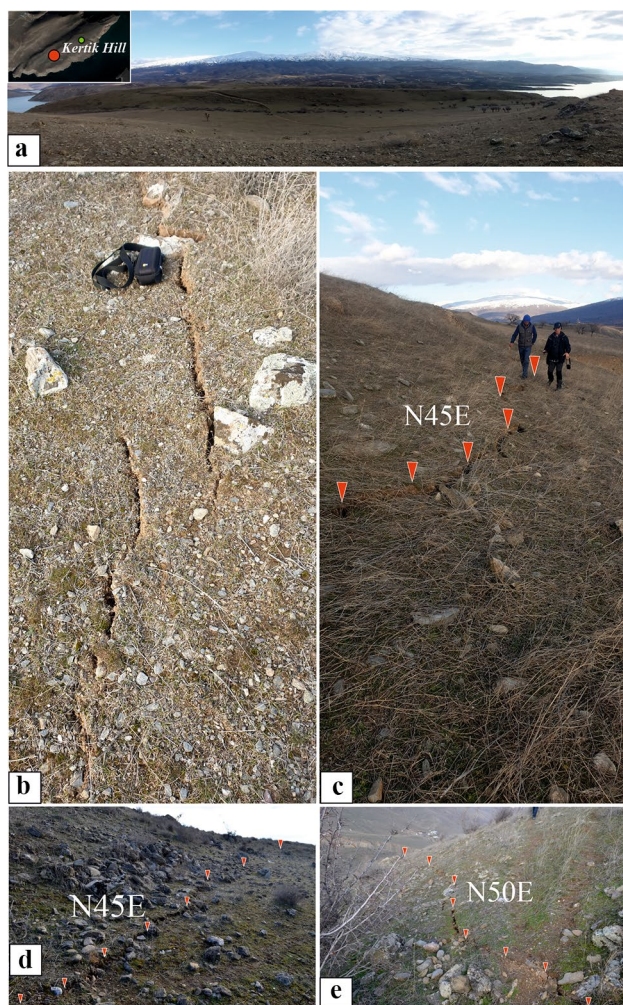


Fig. 11 **a** GoogleEarth image showing the location of surface cracks around the Kertik Hill and Ilıncak village. **b, e** Close-up field views illustrating surface rupture/cracks along the Kertik Hill

50 km (Fig. 16b). In many published articles, data on horizontal deformations were obtained using optical, InSAR, and geodetic data. If we briefly talk about these studies; modeling of geodetic data by Cheloni and Akıncı (2020) obtained from the geodetic inversion shows left-lateral strike-slip with up to 2.3 m of slip. Pousse-Beltran et al. (2020) investigated horizontal surface deformation using an optical image correlation (OIC) of pre-earthquake and post-earthquake maps. Displacement measurement uncertainties are ~ 0.75 m in the east-west component and ~ 1.0 m in the north-south component, whereas WSW of the epicenter, after slip decreases rapidly to $\sim 2\text{--}3$ cm and the locking depth diminishes to near 0, indicating post-seismic surface rupturing (Pousse-Beltran et al. 2020). Jamalreyhani et al. (2020) estimated a uniform slip of 1.6 ± 0.2 m, within 68% of confidence. Melgar et al. (2020) mapped LOS displacements from InSAR showing 45-cm left-lateral sense of slip.

5 Discussion on surface deformation of instrumental earthquakes in Turkey

In this section, classification of surface deformations developed during the instrumental earthquakes in Turkey will be presented and their relation to co- to post-seismic events will be discussed (Table 4; Fig. 17).

As can be seen from the Table 4, ten surface rupture forming earthquakes have occurred on the North Anatolian Fault Zone during the 80-year period between 1939 and 2020. Among these catastrophic events, the maximum magnitude was M_w : 7.9 (1939 Erzincan earthquake), and the minimum magnitude, M_w : 6.8 (1992 Erzincan earthquake) with 360-km-long and 30-km-long surface ruptures, respectively. In these shallow-focus earthquakes, co-seismic earthquake duration varies between 52 and 15 s. The maximum horizontal-slip recorded is 750 cm (December 26, 1939 Erzincan earthquake) and the minimum, 30 cm (August 19, 1966 Varto earthquake). In addition, in the March 13, 1992 Erzincan earthquake, which occurred in a similar magnitude with the Varto Earthquake, 100-cm horizontal slip and 10 cm vertical throw were measured. Considering the earthquakes that resulted in the surface faulting of the last 80 years, it is seen that there is a linear relationship between the earthquake duration and the surface rupture length. Accordingly, while the seismic shaking lasted 52 s (1939 Erzincan earthquake), a 360-km-long earthquake surface rupture developed, while 15 s seismic shaking (1992 Erzincan earthquake), a 30-km-long earthquake surface rupture developed.

When within plate faults examined in Turkey, 48-km-long surface rupture was developed along the Çaldıran fault during the November 24, 1976 Çaldıran earthquake (Toksöz et al. 1977). On the other hand, there is no observed evidence of surface rupture formation during magnitude 6.3 (M_w) earthquake in 1998 along the Misis Fault (Gürsöy et al. 1998). Whereas a 10-km-long surface rupture developed along the Dodurga Fault during the June 6, 2000 Orta-Çankırı earthquake (M_w : 6.0) (Koçyiğit et al. 2001a, b). Similarly, although the 38-km-long surface rupture developed in the 1971 Bingöl earthquake (M : 5.9–6.5) on the East Anatolian Fault Zone, there is no observed evidence (except for a few places) for surface rupturing during the 24 January, 2020 Sivrice (Elazığ)–Doğanyol (Malatya); instead there is overwhelming evidence for occurrence of surface deformation features at regular intervals in approximate 30-km-long deformation zone.

Considering the earthquakes developing in the last century in the contractional tectonic setting, a 28-km-long surface rupture developed on BSZ in the September 6, 1975 Lice earthquake, which lasted for 23 s, there was, however, no significant surface ruptures in the October 23, 2011 Van earthquake, whose magnitude was 7.2 and the duration was

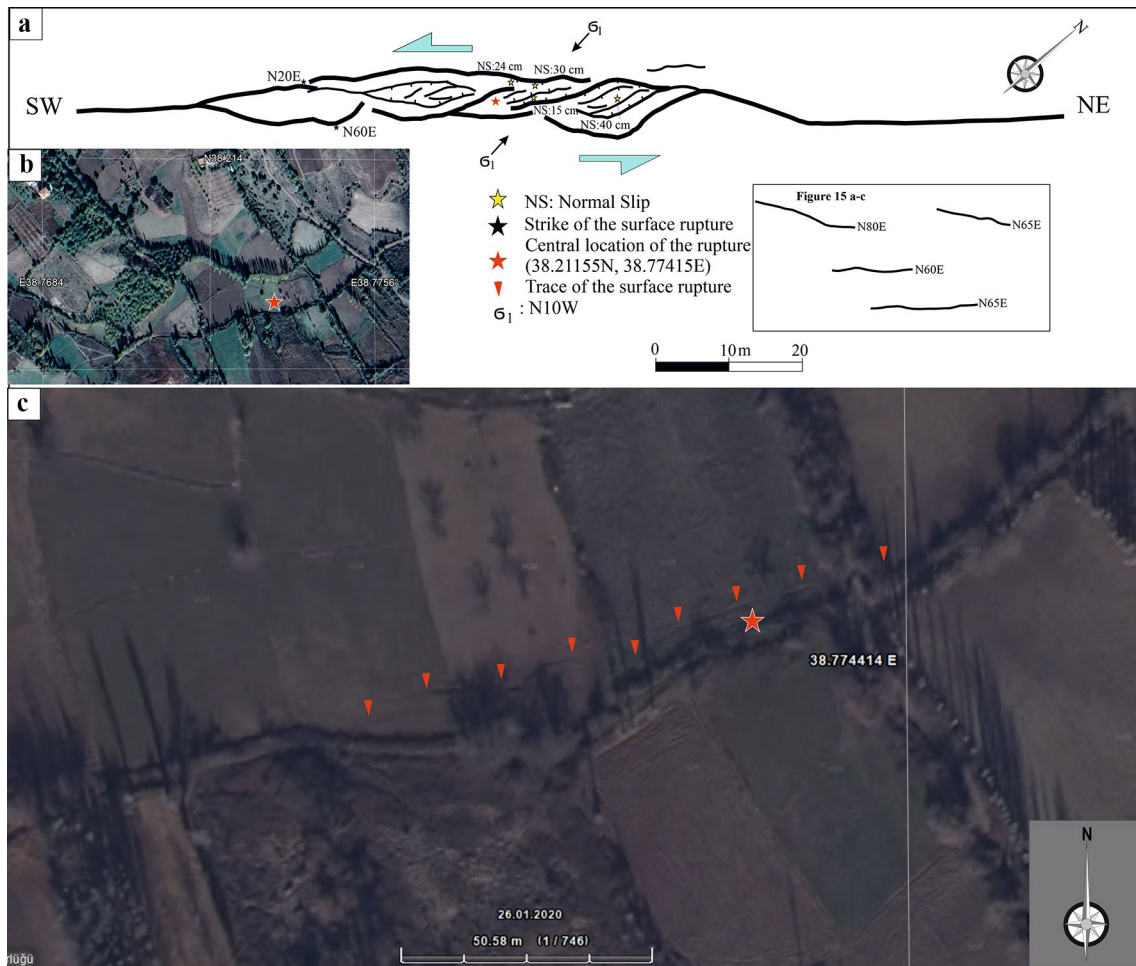


Fig. 12 Structural map of fractures and GoogleEarth image showing surface deformation developing in the form of a large deformation zone to the southwest of Ormaniçi village

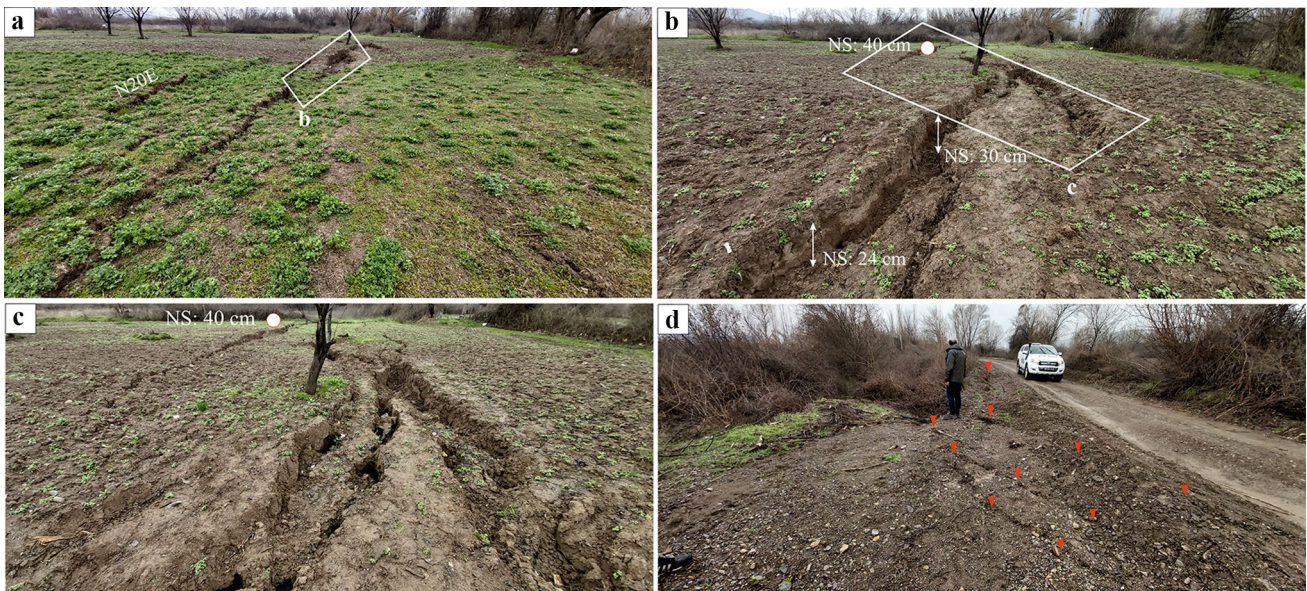


Fig. 13 Field views showing normal-slip motion along individual fractures in a deformation zone to 500 m southwest of Ormaniçi village. Vertical normal slip here reaches up to 40 cm. Views are from southwest to northeast

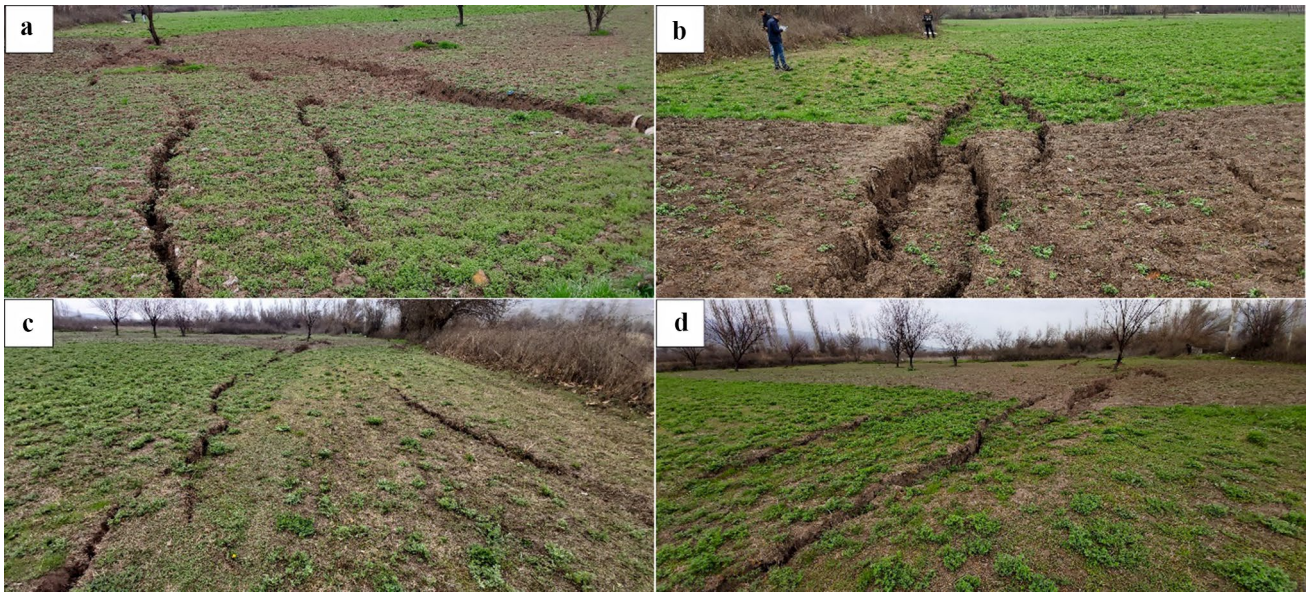


Fig. 14 Different views from surface deformation features observed in the southwest of Ormaniçi village; views are from northeast to southwest

Fig. 15 Different views from surface deformation features observed in the southwest of Ormaniçi village

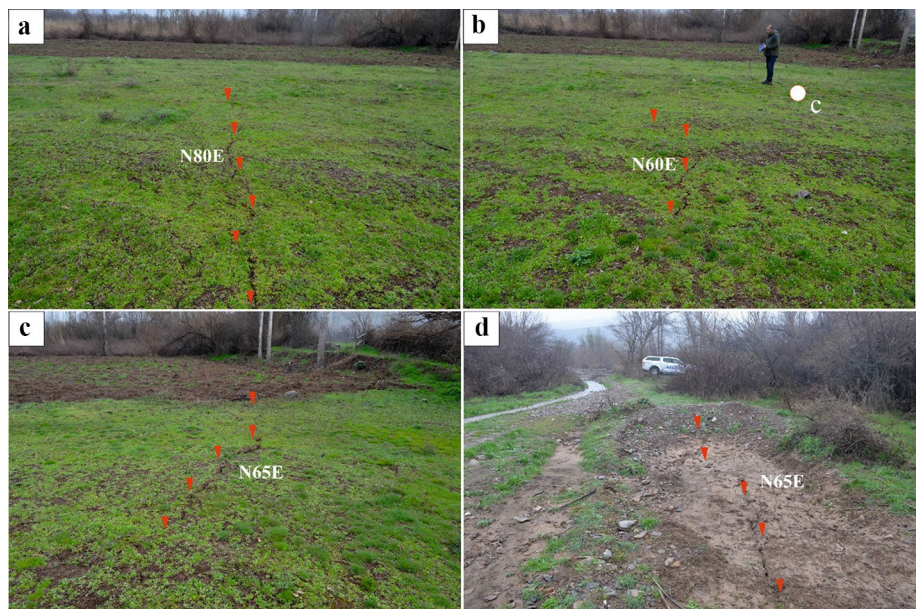


Table 3 S-1 images used for this study

Satellite	Track	Master image	Slave image	Perpendicular baseline (m)	Btemp (days)	Pair type
Sentinel-1A Descending	123	16/01/2020	28/01/2020	58.14	12	Co-seismic
Sentinel-1A Ascending	116	21/01/2020 (1B)	27/01/2020 (1A)	- 39.14	6	Co-seismic
Sentinel-1B Ascending						

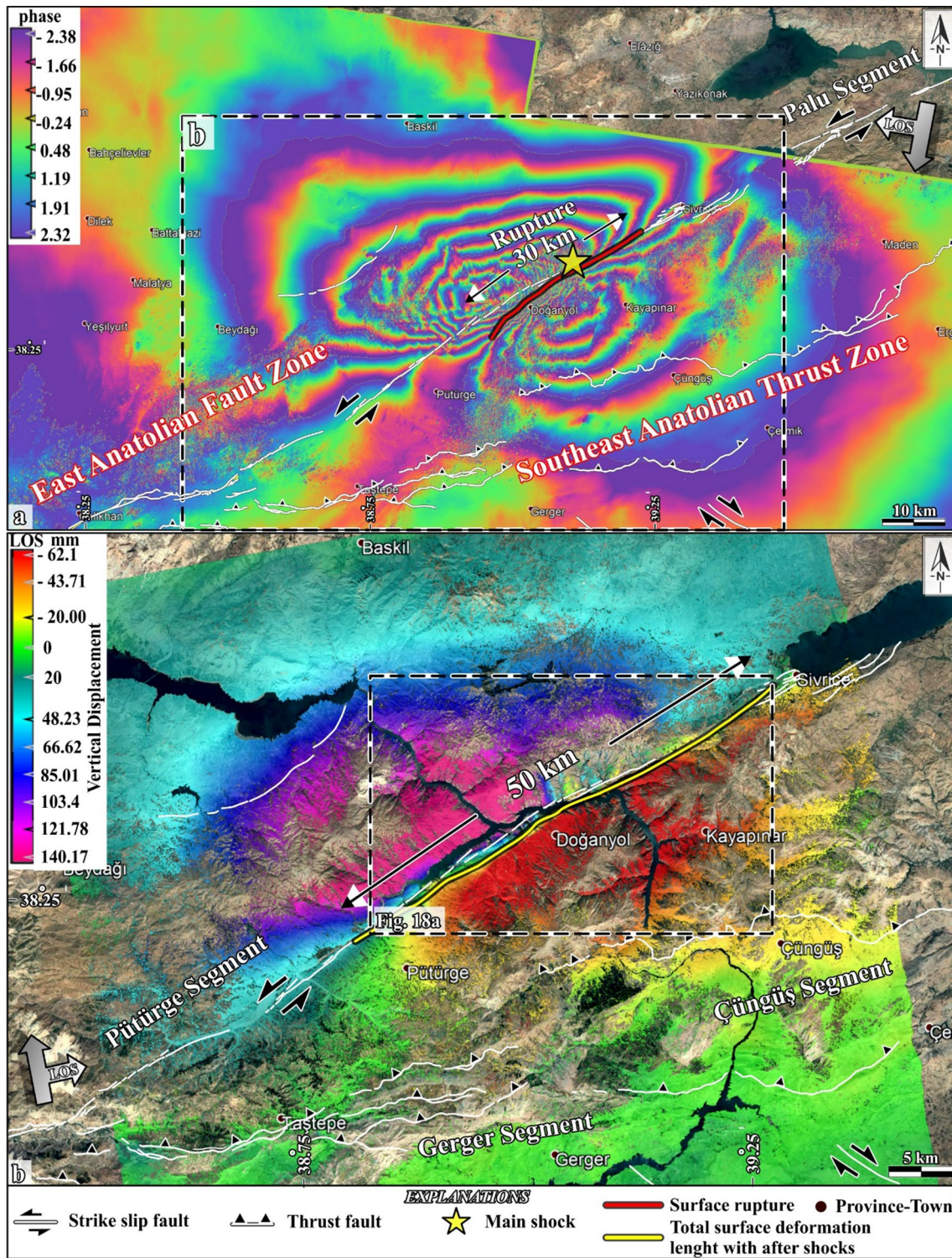


Fig. 16 Co- and post-seismic interferogram maps from the descending tracks. **a** Phase map between 16–28/01/2002 dates and **b** vertical LOS displacement map between 21–27/01/2020 dates. Faults are from Duman et al. (2017); yellow star shows main shock location

29 s. The absence of surface rupture(s) is attributed to the geometry of a blind thrust (Özkaymak et al. 2011).

Similar comparison is made for normal fault earthquakes occurred in western Anatolian extensional province. For example, the February 3, 2002 Çay earthquake ($M=6.0$)

Table 4 Classification of surface deformations of instrumental earthquakes in Turkey between 1939 and 2020

Instrumental Earthquake	Date/time	Depth of hypocenter (km)/magnitude	Co-seismic duration (s)	Surface rupture length/width (km/m)	Name of seismic source/segment	Maximum offset (cm) at the surface			Tectonic setting: strike slip/extensional/compressional	Seismotectonic deformation			Source		
						SS	RS	NS		SR	U/S	PR		MM	LF
Sivrice (Elazığ)–Doğanyol (Malatya)	24 January 2020/20.55	8.06/6.8	22	30/100	EAFZ/ Pütürge segment			40	Strike-slip	+	+	+	+	+	76
Erzincan	26 December 1939/01.57	20/7.9	52	360/	NAFZ/ Erzincan, Suşehri, Reşadiye, Ezinepazar	370–750	–	100–200	Strike-slip	+	+	+	+	+	1, 2, 3,
Erbaa-Niksar	20 December 1942/16.03	10/7.1	30	50/	NAFZ/ Niksar, Erbaa	160–200	–	50–100	Strike-slip	+		+		+	1, 2, 3,
Tosya	26 November 1943/00.20	10/7.6	20	280/	NAFZ/ Destek, Havza, Köprübaşı, Kamil, Kargı, Ilgaz	450–600			Strike-slip	+	+	+	+	+	1, 61, 62, 63
Bolu-Gerede	1 February 1944 / 05.22	10/7.3		165/	NAFZ/Bayramören, İsmetpaşa, Gerede, Bolu	100–350		100	Strike-slip	+	+	+	+		1, 17
Karlıova	17 August 1949 / 20.44	40(28)/6.9 (Ms)		38	NAFZ Elmalidere segment	150		30	Strike-slip	+		+		+	23, 33, 44, 26, 27, 21
Yenice-Gönen	18 March 1953/19.06	10/7.2		70	Yenice-Gönen Fault	170–320		10–50	Strike-slip	+		+	+	+	73, 74, 75
Abant	26 May 1957/08.33	10–14.5/7.0		30	NAFZ	140–160		40	Strike-slip	+		+		+	1, 64
Varto	19 August 1966 / 14.22	26 (26)/6.8 (Ms) 6.8 (Mw) (39) 6.7 (Mw) (42)	30	34/5	NAFZ Varto segment	30		25	Strike-slip	+		+	+	+	23, 25, 33, 49, 51, 59, 26, 22, 21, 53
Mudurnu Valley	22 July 1967/18.56	5/7.1, 6.8 Ms		80	NAFZ	140–260			Strike-slip	+		+	+	+	1, 65

Table 4 (continued)

Instrumental Earthquake	Date/time	Depth of hypocenter (km)/magnitude	Co-seismic duration (s)	Surface rupture length/wide (km/m)	Name of seismic source/segment	Maximum offset (cm) at the surface			Tectonic setting: extensional/compressional	Seismotectonic deformation			Source	
						SS	RS	NS		SR	U/S	PR		MM
Alaşehir	28 March 1969/03.48	4/Mw: 6.1, Ms:6.5	28	36/	Gediz Graben/Alaşehir			3–13	Extensional	+	+	+	+	4, 5, 6
Gediz	28 March 1970 / 23.02	18 (28), 33 (43)/7.1(Ms) 7.0 (Mw) (40) 7.1 (Mw) (41) 6.8 (Mw) (39)	6 (wikipedia)	45	Gediz fault	30	230		Extensional	+				23, 24, 36, 41, 54, 26, 27, 21, 35, 32, 43, 46, 50
Bingöl	22 May 1971 / 18.43	3(28), 10 ± 2(27)/ 6.8(Ms) 6.5 (Mw)(39) 5.9 (Mw) (27) 6.3 (Mw) (38)		38	EAFZ	60	10		Strike-slip	+	+	+		23, 28, 30, 45, 52, 26, 55, 27, 21, 34
Lice	6 September 1975/12.20	31.9(28)/6.6(Ms) 6.2(Mw)(37) 6.4(Mw)(38)	23	28	BSZ	60	60		Compressional	+	+	+		23, 29, 42, 56, 26, 27, 21, 48, 34
Muradiye	24 November 1976/14.22	8.60(29) 10(30)/7.3 (Ms) 7.3 (Mw)(31) 6.7 (Mw) (15) 6.9 (Mw) (39)		48	Çaldıran fault	350	50		Strike-slip	+				23, 31, 33, 38, 42, 56, 57, 26, 40, 39, 58, 21, 35
Erzurum-Kars	30 October 1983/07.12	15(29) 10(30)/6.7 (Ms) 6.8 (Mw)		12	Horasan Narman fault(11, 34,35) Çobandede fault zone (36) [NAFZ]	100	60		Strike-slip	+				23, 38, 26, 40, 39, 21, 32, 37, 47
Erzincan	13 March 1992/19.08	12–29/6.8	15	20–30/	NAFZ, Erzincan	95–100	10		Strike-slip	+	+	+		66, 67, 68
Dinar	1 October 1995/17.57	15/Mw:6.4	25	10/	Dinar Fault	10	50		Extensional	+	+	+		4, 7, 8, 9, 16
Ceyhan	27 June 1998 / 16.55	30/Mw:6.3	20	20 (yüzey kırığı izi gözlenmemiş, tahmini uzunluk)	Misis Fault				Strike-slip		+	+		4, 10, 17

Table 4 (continued)

Instrumental Earthquake	Date/time	Depth of hypocenter (km)/magnitude	Co-seismic duration (s)	Surface rupture length/wide (km/m)	Name of seismic source/segment	Maximum offset (cm) at the surface		Tectonic setting: strike slip/extensional/compressional	Seismotectonic deformation				Source		
						SS	RS NS		SR	U/S	PR	MM		LF	FS
İzmit	17 August 1999/03.01	17/7.4	45	145/1–4 km	NAFZ, Hersek, Karamürsel-Gölcük, İzmit-Sapanca Lake, Sapanca-Akyazi, Karadere	520	- 230	Strike-slip	+	+	+	+	+	+	69
Düzce	12 Novem-ber 1999/18.57	10–18/7.2	30	35–45/1	NAFZ	380–490	76	Strike-slip	+	+	+	+	+	+	70, 71, 72
Orta-Çankırı	6 June 2000/05.41	15/Mw:6.0	10	10/7	Dodurga Fault	1		Strike-slip	+	+	+	+	+	+	4, 13, 14, 18, 19
Çay-Sultandağı	3 February 2002/09.11	15/Mw:6.5	20	21/	Sultandağı Fault/Çay segment		25	Extensional	+	+	+	+	+	+	4, 15, 20
Van	23 October 2011/13.41	19/Mw:7.2	29	No surface rupture				Compressional	+	+	+	+	+	+	11, 12

SR surface rupture, land uplift/subsidence (permanent ground deformation), PR pressure ridge, MM mass movement, FS fissure, LS lateral spreading, LF liquefaction, NAFZ north anatolian fault zone, EAFZ east anatolian fault zone, SS strike-slip, RS reverse slip, NS normal slip

Segment names from Emre, Ö., Duman, T.Y., Özalp, S., Elmacı, H., Olgun, Ş. ve Şaroğlu, F., 2013, Açıklamalı Türkiye Diri Fay Haritası. Ölçek 1:1.250.000, Maden Tetkik ve Arama Genel Müdürlüğü, Özel Yayın Serisi-30, Ankara-Türkiye. ISBN: 978-605-5310-56-1

Sources: (1) Barka, A. (1996). Slip Distribution along the North Anatolian Fault Associated with the Large Earthquakes of the Period 1939 to 1967. Bulletin of the Seismological Society of America, Vol. 86, No 5, pp. 1238–1254. (2) Blumenthal (1943); (3) Pamir and Akyol (1942); (4) Kalafat, D., Güneş, Y., Kekovalı, K., Kara, M., Deniz, P., Yılmaz, M., 2011, A Revised and Extended Earthquake Catalogue for Turkey since 1900 (1900–2010; $M \geq 4.0$), Boğaziçi University Kandilli Observatory and Earthquake Research Institute, İstanbul. (5) Gören, R., 2016, Alaşehir ve Çevresinde Gediz Grabeni Güney Kenar Faylarının Holosen Aktivitesi, Eskişehir Osmangazi Üniversitesi Fen Bilimleri Enstitüsü Jeoloji Mühendisliği Anabilimsel Yürütme Kurulu Yüksek Lisans Tezi, 95 sayfa. (6) Eyidoğan, H., Jackson, J., 1985, A Seismological Study of Normal Faulting in the Demirci, Alaşehir and Gediz Earthquakes of 1969–70 in Western Turkey: Implications for the Nature and Geometry of Deformation in the Continental Crust. Geophys. J. R. astr. Soc., 81, 569–607. (7) Eyidoğan, H., Barka, A., 1996, The 1 October 1995 Dinar Earthquake, SW Turkey. Terra Nova, 8, 479–485. (8) Altunel, E., Barka, A., Akyüz, S., 2002, Palaeoseismicity of the Dinar Fault, SW Turkey, Terra Nova, 1 (6), 297–302. (9) Demirtaş, R., Karakısa, S., Demir, M., İravul, Y., Baran, B., Bağcı, G., Yatman, A., Zinbil, S., Yılmaz, R., 1995, 1 Ekim 1995 Dinar Depremi, Afet İşleri Genel Müdürlüğü Deprem Araştırma Dairesi Başkanlığı, 21 sayfa. (10) Ulusay, R., Aydın, Ö., Kumsar, H., Sönmez, H., 2000, Engineering Geological Characteristics of the 1998 Adana-Ceyhan Earthquake, with Particular Emphasis on Liquefaction Phenomena and the Role of Soil Behaviour. Bulletin of Engineering Geology and the Environment, 59:99–118. (11) Alan, H., Bozkurt, E., Çağlan, D., Dirik, K., Özkaymak, Ç., Sözbilir, H., Topal, T., 2011, Van Depremleri (Tabanlı-Edremit) Raporu, Jeoloji Mühendisleri Odası Yayın No: 110, ISBN: 978-605-01-0210-9. (12) Güneş, D., (Ed.), 2011, Yıldız Teknik Üniversitesi 23 Ekim 2011 Van Depremi Teknik İnceleme Raporu, 62 sayfa. (13) Koçyiğit, A., Rojday, B., Cihan, M., Özacar, A., 2001, The June 6, 2000, Orta (Çankırı, Turkey) Earthquake: Sourced from a New Antithetic Sinistral Strike-Slip Structure of the North Anatolian Fault System, the Dodurga Fault Zone, Turkish Journal of Earth Sciences, Vol. 10, pp. 69–82. (14) Emre, Ö., Duman, T.Y., Dogan, A. and Özalp, S., 2000, 6 Haziran 2000 Orta (Çankırı) Depremi Değerlendirme Raporu, MTA Rapor No:10323, Ankara. (15) Emre, Ö., Duman, T., Doğan, A., Özalp, S., Tokay, F., Kuşçu, İ., 2002, 03 Şubat 2002 Sultandağı Depremi Ön Değerlendirme Raporu, MTA, Ankara. (16) Biricik, A.S., Ceylan, M.A., Ünlü, M., 1996, 1 Ekim 1995 Dinar Depremi, Marmara Coğrafya Dergisi, Year 1998, (2):

Table 4 (continued)

- 95–121, İstanbul. (18) Demirtaş, R., İravul, Y., Erkmen, C., Baran, B., Yaman, M., Baykal, M., Kılıç, T., 2000. Çankırı Depremi 06 Haziran 2000 Orta (Çankır) Depremi. JMO Haber Bülteni 1–2, sayfa 6–15. (19) Emre, Ö., Duman, T.Y., Doğan, A., Özalp, S., 2000. Haziran 2000 Orta (Çankır) Depremi Yine mi KAF?, TÜBİTAK Bilim ve Teknik Dergisi, Temmuz, 18–21. (20) Akyüz, H.S., Uçar, G., Şatır, D., Dikbaş, A., Kozacı, Ö., 2006. 3 Şubat 2002 Çay Depreminde Meydana Gelen Yüzey Kinği Üzerinde Paleoseismolojik Araştırmalar, Yerbilimleri Hacettepe Üniversitesi Yerbilimleri Uygulama ve Araştırma Merkezi Dergisi, 27(1), 41–52. (21) AFAD: Başbakanlık Afet ve Acil Durum Yönetimi Başkanlığı, Deprem Dairesi Kataloğu, 2007–2012 <https://www.deprem.gov.tr/sarbis/Veritabanı> (22) Ahsan, E., Tezuçan, L. & Bath, M. (1975). An earthquake catalogue for Turkey for the interval 1913–1970. Kandilli Observatory Seismological Department C, engelko y-İstanbul, Turkey and Seismological Institute Box 517, S-751 20 Uppsala, Sweden. (23) Ambraseys, N. (1988). Engineering Seismology. J. Earthq. Eng. Struct. Dyn., 17, 1–106. (24) Ambraseys, N. & Tchalenko, J. (1972). Seismotectonic aspects of the Gediz earthquake of March 1970. Geophys. J. R. astr. Soc., 30, 229–252. (25) Ambraseys, N. & Zatopek, A. (1968). The Varto Usukran earthquake of 19 August 1966. Bulletin of the Seismological Society of America, 58, 47–102. (26) Ambraseys, N. & Jackson, J.A. (1998). Faulting associated with historical and recent earthquakes in the Eastern Mediterranean region. Geophys. J. Int., 133, 390–406. (27) Ayhan, E., Ahsan, E., Sancaklı, N. & Üçer, S.B. (1981) Turkey and surrounding earthquake catalogue 1881–1980. Boğaziçi University Publications, İstanbul. (28) Arpat, E. (1971). 22 Mayıs 1971 Bingöl depremi: Ölü Deniz fay sisteminin Karlıova ilçesi ile Hazar Gölü arasındaki bölünümü. Report MTA, Ankara. (29) Arpat, E. (1977). 1975 Lice depremi. Yeryuvarı ve İnsan, 2, 15–27. Ankara. (30) Arpat, E. & Şaroğlu, F. (1972). The East Anatolian Fault system: thoughts on its development. Bulletin Mineral. Explor. Inst., no. 78, 33–39. Ankara. (31) Arpat, E., Şaroğlu, F. & İz, H. (1977). 1976 Çaldıran depremi. Yeryuvarı ve İnsan, 2, 29–41. Ankara. (32) Barka, A.A., Şaroğlu, F. & Güner, Y. (1983). 1983 Horasan-Narman earthquake and its place in the neotectonics of eastern Turkey. Yer Yuvarı ve İnsan, 8, 16–21. (33) Barka, A. & Kadinsky-Cade, K. (1988). Strike-slip fault geometry and its influence on earthquake activity in Turkey. Tectonics, 3, 663–684. (34) EMMA: G. Vannucci and P. Gasperini. (2004) The new release of the database of Earthquake Mechanisms of the Mediterranean Area (EMMA version 2), Annals of Geophysics, Supplement to Vol 47, 303–327. (35) Duman, T.Y., Çan, T., Emre, Ö., Kadıroğlu, F.T., Başarır Baştürk, N., Kılıç, T., Arslan, S., Kartal, R.F., Kalafat, D., Karakaya, F., Eroğlu Azak, T., Öznel, N.M., Ergintav, S., Akkar, S., Altınok, Y., Tekin, S., Cingöz, A. & Kurt A.İ. (2016). Seismotectonic database of Turkey; Bulletin of Earthquake Engineering, 16(8), 3277–3316. (36) Eyidoğan, H. & Jackson, J. (1985). A seismological study of normal faulting in the Denizci, Alaşehir and Gediz earthquakes of 1979–7 in western Turkey: implications for the nature and geometry of deformation in continental crust. Geophys. J. R. astr. Soc., 81, 569–607. (37) Eyidoğan, H., Nalbant, S.S., Barka, A. & King, G.C.P. (1999). Static stress changes induced by the 1924 Pasinler (M=6.8) and 1983 Horasan-Narman (M=6.8) earthquakes, Northeastern Turkey. Terra Nova, 11, 38–44. (38) Gülkan, P., Gürpınar, A., Çelebi, M., Arpat, E. & Gençoğlu, S. (1978). Engineering report on the Muradiye-Çaldıran, Turkey, earthquake of 24 November 1976. Publ. Natl. Res. Council. Natl. Akad. Sci., Washington, DC. (39) HRVD-GCMT: The Harvard Centroid-Moment-Tensor Catalog. <https://www.isc.ac.uk/isbulletin/search/catalogue/> (41) Jackson, J. & Fitch, A. (1979). Seismotectonic implications of relocated aftershock sequence in Iran and Turkey. Geophys. J. R. astr. Soc., 57, 209–229. (42) Jackson, J. & McKenzie, D. (1984). Active tectonics of the Alpine–Himalayan Belt between western Turkey and Pakistan. Geophys. J. R. astr. Soc., 77, 185–264. (43) Jackson, J., Haines, J. & Holt, W. (1992). The Horizontal Velocity Field in the Deforming Aegean Sea Region Determined from the Moment Tensors of Earthquakes. J. Geophys. Res., Vol. 97, N. B12, 17,657–17,684. (44) Kadinsky-Cade, K. & Barka, A. (1989). Relationship between restraining bends and earthquake magnitude: large earthquakes in strike-slip zones. USGS Workshop Fault Segment & Controls, Open File Rept no. 89/315, 181–192. (45) Keightly, W. (1975). Destructive earthquakes in Burdur and Bingöl, Turkey. Publ. Natl. Acad. Sci., Washington, DC. (46) Kirazlı, A. & Louvari, E. (2003). Focal mechanisms of shallow earthquakes in the Aegean Sea and the surrounding lands determined by waveform modelling: a new database. Journ. of Geodyn., 36, 251–274. (47) Koçyiğit, A., Yılmaz, A., Adamiya, S. & Kuloshvili, S. (2001). Neotectonics of East Anatolia plateau (Turkey) and lesser Caucasus: implication for transition from thrusting to strike-slip faulting. Geodinamica Acta, 14, 177–195. (48) KOERI: Boğaziçi Üni. Kandilli Rasathanesi ve Deprem Araştırma Enstitüsü Kataloğu 2011–2012 <https://udim.koeri.boun.edu.tr>. (49) Kudo, K. (1983). Seismic source characteristics of recent major earthquakes in Turkey. Comprehensive Study of Earthquakes in Turkey. Publ. Eng. Faculty, Hokkaido University, Sapporo. (50) Mckenzie, D. (1978). Active Tectonics of the Alpine-Himalayan Belt: the Aegean Sea and Surrounding Regions. Geophys. J. R. Astr. Soc., 55, 217–254. (51) North, R.G. (1977). Seismic moment, source dimensions and stress associated with earthquakes in the Mediterranean and Middle East. Geophys. J. R. astr. Soc., 48, 137–161. (52) Seymen, I. & Aydın, A. (1972). The Bingöl earthquake fault and its relation to the North Anatolian fault zone. Bull. Mineral. Res. Explor. Inst., no. 79, 1–8. Ankara. (53) Steward, G.S. & Kanamori, H. (1982). Complexity of rupture in large strike-slip earthquakes in Turkey. Phys. Earth Planet. Int., 28, 70–84. (54) Taşdemiroğlu, M. (1971). The Gediz earthquake in Western Anatolia Turkey. Bull. seism. Soc. Am., 61, 1507–1527. (55) Taymaz T., Jackson J. & McKenzie, D. (1991). Active Tectonics of the North and Central Aegean Sea. Geophys. J. Int., 106, 433–490. Tay. GJI1991a. (56) Toksöz, M.N., Arpat, E. & Şaroğlu, F. (1977). East Anatolian earthquake of 24 Nov. 1976; field observations. Nature, 270, 423–25. (57) Toksöz, M.N., Nabelek, N. & Arpat, E. (1978). Source earth properties of the 1976 earthquake in east Turkey: a comparison of field data and teleseismic results. Tectonophysics, 49, 199–205. (58) USGS: United States Geological Survey, Amerika. (59) Wallace, R. (1968). Earthquake of August 19, 1996. Varto area, Eastern Turkey. Bull. seism. Soc. Am., 58, 11–56. (60) Emre, Ö., Kondo, H., Yıldırım, C. & Özaksay, V. (1) Kuzey Anadolu Fayı 1943 Tosya Depremi Yüzey Kinği. Türkiye Jeoloji Kurultayı, Bildiri Özleri Kitapeği, s. (61) Yoshioka, T., Okumura, K., Kuşçu, İ., Emre, Ö., 2000. Recent surface faulting of the North Anatolian Fault along the 1943 Ladik earthquake ruptures. Bull. Geol. Survey. Jpn., 51(1), 29–35. (62) Fraser, J., Pigati J.S., Hubert-Ferrati, A., Vanneste, K., Aysar, U., Altınok, S. 2009. A 3000-year record of groundrupturing earthquakes along the Central North Anatolian Fault near Lake Ladik, Turkey. Bull. of the Seis. Soc. of America, 99, 2681–2703. (63) Hartleb, R.D., Dolan, J.F., Akyüz, H.S., Yerli, B. 2003. A 2000-year-long paleoseismologic record of earthquakes along the central North Anatolian Fault, from trenches at Alayurt, Turkey. Bull. of the Seis. Soc. of America, 93, 1935–1954. (64) Öcal, N., 1959. 26 Mayıs 1957 Abant Zelvelesi, İstanbul Kandilli Rasathanesi, Sismoloji Yayınları:4, İstanbul. (65) Kalafatçıoğlu, A. (1967). 22 Temmuz 1967 Sakarya Depremine Ait Rapor, MTA Rapor No 3872, Ankara. (66) Barka, A. and Eyidoğan, H. The Erzincan earthquake of 13 March 1992 in eastern Turkey. Terra Nova, Vol.5, Issue 2, p.190–194. (67) Tatar, O., Temiz, H., Tutkun, S.Z., Park, R.G. and Stimpson, I.G. 1993. Surface deformation and tectonic setting of the 13 March 1992 Erzincan earthquake, eastern Turkey. Geological Journal, Vol. 28, Issue 3–4, p. 327–333. (68) Barka, A. 1993. Erzincan baseni çevresinin tektoniği ve 13 Mart 1992 Depremi. İnşaat Mühendisleri Odası, 2. Ulusal Deprem Mühendisliği Konferansı, Bildiriler Kitabı, s.259–270. (69) A. Barka, H. S. Akyüz, E. Altınel, G. Sunal, Z. Çakır, A. Dikbaş, B. Yerli, R. Armijo, B. Meyer, J. B. de Chaballier, T. Rockwell, J. R. Dolan, R. Hartleb, T. Dawson, S. Christofferson, A. Tucker, T. Fumal, R. Langridge, H. Stenner, W. Lettis, J. Bachhuber, and W. Page. 2000. The Surface Rupture and Slip Distribution of the 17 August 1999 Izmit Earthquake (M 7.4), North Anatolian Fault. Bulletin of the Seismological Society of America, 92, 1, pp. 43–60. (70) M. E. Ayhan, I. R. Bfingmann, 2 S. McClusky, 30. Lenk, Herece, 4 and R. E. Reilinger (2001). Kinematics of the Mw = 7.2, 12 November 1999, Düzce Earthquake. Geophysical Research Letters, Vol. 28, No. 2, p. 367–370. (71) H. S. Akyüz, R. Hartleb, A. Barka, E. Altınel, G. Sunal, B. Meyer, R. Armijo. 2002. Surface Rupture and Slip Distribution of the 12 November 1999 Düzce Earthquake (M 7.1), North Anatolian Fault, Bolu, Turkey. Bulletin of the Seismological Society of America, 92 (1): 61–66. (72) Özden, S., Tatar, O., Mesci, B.L., Koçbulut, F., Tutkun, S.Z. Doğan, B., Tüvar, O. 2000. 12 Kasım 1999 Düzce Depremi ve Bölgesel Tektonik Anlamı. Türkiye

Table 4 (continued)

Jeoloji Bülteni, C.43, S.2, s.61–69. (73) Kürçer, A., Chatzipetros, A., Tutkun, S. Z., Pavlides, S., Ateş, Ö., Valkaniotis, S. 2008. The Yenice–Gönen active fault (NW Turkey): Active tectonics and palaeoseismology. *Tectonophysics*, 453, 263–275. (74) Kürçer, A., Özalp, S., Özdemir, E., Uygun Güldoğan, Ç., Duman, T. Y. 2019. Active tectonic and paleoseismologic characteristics of the Yenice–Gönen Fault, NW Turkey, in light of the 18 March 1953 Yenice–Gönen Earthquake ($M_s=7.2$). *Bulletin of Mineral Research and Exploration*, 159, 29–63. <https://dx.doi.org/10.19111/bulletinofmre.500553>. (75) Keim, I., Roesly, F. 1953. Makroseismische Untersuchungen über das nordwestanatolische Beben vom 18. März 1953. *Eclogae Geol. Helv.* 46, 187–208. (76) Tatar, O., Sözbilir, H., Bozkurt, E., Aksoy, E., Koçbulut, F., Özmen, B., Alan, H. ve Metin, Y. 24 Ocak 2020 Sivrice (Elazığ)–Doğanyol (Malatya) Depremi: Arazi Gözlemleri ve Değerlendirilmesi. TMMOB Jeoloji Mühendisleri Odası, Yayın No 145, 82 s

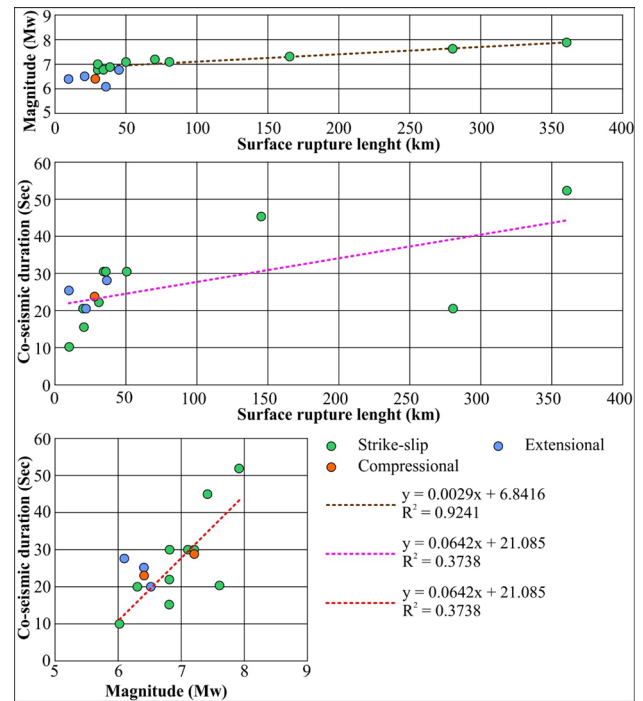


Fig. 17 a and b Relationship between surface rupture length and magnitude/co-seismic duration and c magnitude and co-seismic duration of strike slip/compressional/extensional earthquakes that developed during the last hundred years in Turkey

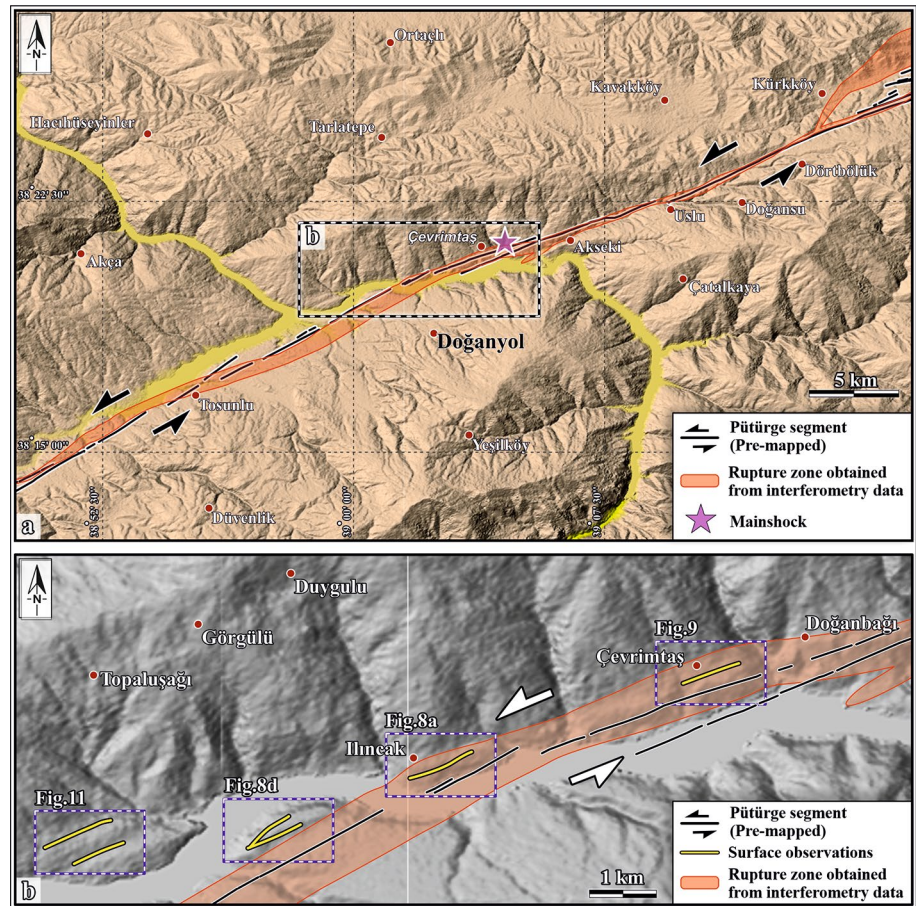
lasted for 21 s and developed a 21-km-long surface rupture on Sultandağı Fault. In addition, during the October 1, 1995 Dinar earthquake (M_w : 6.2), which lasted 25 s, a 10-km-long surface rupture was mapped. The seismic shaking of M_w : 6.5 magnitude event lasting 28 s in the March 28, 1969 Alaşehir earthquake resulted in the development of a 36-km-long surface rupture. A 45-km-long surface rupture developed on the Gediz Fault during the March 28, 1970 Gediz earthquake with a magnitude M_w : 6.8–7.1. Accordingly, it is suggested that surface ruptures form during normal fault earthquakes with magnitudes M_w : 6.0 and larger in extensional environments.

On the other hand, surface deformations related to seismic shaking develop in all earthquakes with a magnitude larger than 6.0 and this totally depends on local ground conditions and groundwater level as being close to the surface. The mass movements triggered by the earthquake are, however, related to the lithological and structural features of the units that outcrop along the fault zone and the presence of critical slopes that are stable at a certain critical angle.

6 Conclusion

Discontinuous surface deformation features occur within an approximately 30-km-long and 200–300 m wide deformation zone during the Sivrice (Elazığ)–Doğanyol (Malatya)

Fig. 18 **a** DEM map showing the relationship between the surface rupture obtained with interferometric data and the previously mapped Pütürge segment. **b** Surface deformations obtained by field observations and interferometric rupture zone



earthquake. The deformation zone width obtained from interferometry is, however, approximately 1 km (Fig. 18). The observed and mapped seismic geomorphological deformation and related features in the area between Gezin (Elâzığ) and Ormaniçi (Pütürge) villages are classified into two classes as seismotectonic and seismo-gravitational features. Surface rupture and cracks, uplifted and subsiding topography and elongated pressure ridges are common seismotectonic surface features while mass movements, lateral spreading and liquefaction are reported as seismo-gravitational surface features.

Although no significant strike-slip displacement was observed along the surface fractures, vertical offsets up to 40 cm were measured, especially in the southwest of Ormaniçi village. The absence of a regular surface fractures as a result of the 6.8 magnitude earthquake can be explained in different ways: (1) left-lateral strike-slip displacement was not able to reach the surface; (2) left-lateral torque movement of the fault around a vertical axis during the earthquake, (3) restraining bend nature of the Pütürge Segment, or (4) the presence of Pütürge metamorphics along the fault strike. It is also important to note that

along most part of the Pütürge segment, surface deformation features are observed in areas where talus, colluvial or alluvial fan sediments are exposed. Unconsolidated and/or poorly consolidated nature of these sediments may also be counted as one of the main reason for not observing horizontal displacements on the surface. The fracture passes through the metamorphic rocks of the Pütürge Massif in the region. The earthquake increased the stress level on the southwestern end of the Pütürge segment and the adjacent Palu segment to the northeast. It has been observed that previously mapped Pütürge segment and field observations show a deformation pattern consistent with interferometry data (Fig. 18b).

Earthquakes with magnitudes 6.0 and larger that occurred on different active faults of Turkey in the last century are examined in terms of surface deformations. It is clearly seen that most were not associated with regular surface ruptures. Specifically, the earthquakes associated with strike-slip faulting along the North and East Anatolian Fault Zones create surface ruptures with magnitudes 6.0 and larger. It is, therefore, concluded that (1) the formation of the surface deformations varied according to the fault type and the state

of regional stress in a given region, (2) the magnitude of the earthquake, (3) the duration time of the earthquake and (4) the geomorphologic feature of landscape in relation to the lithologic and structural features of the rock units located along the active fault zone.

Acknowledgements We would like to thank the Chamber of Geological Engineers, AFAD Sivas Provincial Directorate, Elazığ Police House, and Pertek Mayor Ruhan Alan for their logistics support for the realization of this work. Thanks to İsmail Duran for his help in drawing Fig. 3.

References

- Afet ve Acil Durum Yönetimi Başkanlığı (AFAD) Deprem Dairesi Başkanlığı (2020) 24 Ocak 2020 Sivrice (Elazığ) Mw 6.8 Depremine İlişkin Ön Değerlendirme Raporu. 9 s. <https://depre.m.afad.gov.tr/downloadDocument?id=1825>. Accessed 20 July 2020
- Aksoy E, Inceoz M, Koçyiğit A (2007) Lake Hazar basin: a negative flower structure on the East Anatolian fault system (EAFS), SE Türkiye. *Turk J Earth Sci* 16:319–338
- Aktuğ B, Özener H, Dogru A, Sabuncu A, Turgut B, Halıcıoğlu K, Yılmaz O, Havazlı E (2016) Slip rates and seismic potential on the East Anatolian Fault System using an improved GPS velocity field. *J Geodyn* 94–95:1–12
- Aktimu HT, Oral A (1981) Şiro çayı ve dolayının yerbilim verileri. Institute of Mineral Research and Exploration Report, 6883, Ankara
- Ambraseys N (1988) Engineering seismology. *J Earthq Eng Struct Dyn* 17:1–106
- Ambraseys NN, Jackson J (1998) Faulting associated with historical and recent earthquakes in the eastern Mediterranean region. *Geophys J Int* 133:390–406
- Ambraseys NN, Finkel C (1995) Seismicity of Turkey and neighbouring regions 1500–1800. *Geophys J Int* 133:390–406
- Arpat E, Şaroğlu F (1972) Doğu Anadolu Fayı ile ilgili bazı gözlemler ve düşünceler. Maden Tetkik ve Arama Enstitüsü, Ankara, pp 44–50
- Arpat AE, Şaroğlu F (1975) Türkiye’de bazı önemli genç tektonik olaylar. *Türkiye Jeoloji Kurumu Bülteni* 18:29–41
- Audemard FA, De Santis F (1991) Survey of liquefaction structures induced by recent moderate earthquakes. *Bull Int Assoc Eng Geol* 44:5–16
- Baştürk NB, Özel NM, Altınok Y, Duman TY (2017) Türkiye ve yakın çevresi için geliştirilmiş tarihsel dönem (MÖ 2000–MS 1900-) deprem kataloğu. In: Duman TY (ed) Türkiye Sismotektonik Haritası Açıklama Kitabı, Özel Yayınlar Serisi 34. Maden Tetkik ve Arama Genel Müdürlüğü, Ankara, p 239
- Boğaziçi Üniversitesi Kandilli Rasathanesi ve Deprem Araştırma Enstitüsü Deprem Mühendisliği Ana Bilim Dalı (2020) 24 Ocak 2020 (20:55) Elazığ-Sivrice Depremi Sismotektonik Yapı, Kuvvetli Deprem Yer Hareketi Dağılım Özellikleri ve Bina Hasar Tahminleri Ön Rapor, 20 s
- Bulut F, Bohnhoff M, Eken T, Janssen C, Kılıç T, Dresen G (2012) The East Anatolian Fault Zone: seismotectonic setting and spatiotemporal characteristics of seismicity based on precise earthquake locations. *J Geophys Res* 117(B07304):1–16
- Çelik H (2008) Doğu Anadolu Fay Sistemi’nde Sivrice Fay Zonu’nun Palu-Hazar Gölü (Elazığ) Arasındaki Bölümünde Atımla İlgili Yeni Arazi Bulgusu. *F.Ü. Fen ve Mühendislik Bilimleri Dergisi* 20(2):305–314
- Çetin H, Güneyli H, Mayer L (2003) Paleosismology of the Palu-Lake Hazar segment of the East Anatolian Fault Zone, Turkey. *Tectonophysics* 374:163–197
- Cheloni D, Akıncı A (2020) Source modelling and strong ground motion simulations for the 24 January 2020, M w 6.8 Elazığ earthquake, Turkey. *Geophys J Int* 223(2):1054–1068
- Çolak S, Aksoy E, Koçyiğit A, İnceöz M (2012) The Palu-Uluova Strike-Slip Basin in the East Anatolian fault system, Turkey: its transition from the Palaeotectonic to Neotectonic Stage. *Turk J Earth Sci* 21:547–570
- Dewey JF, Hempton MR, Kidd WSF, Şaroğlu F, Şengör AMC (1986) Shortening of continental lithosphere: the neotectonics of eastern Anatolia: a young collision zone. In: Coward MP, Ries AC (eds) *Collision tectonics*, 19th edn. Geological Society, London, pp 3–36
- Dramis F, Blumetti AM (2005) Some considerations concerning seismic geomorphology and paleoseismology. *Tectonophysics* 408(1–4):177–191
- Duman TY, Emre Ö (2013) The East Anatolian Fault: geometry, segmentation and jog characteristics. In: Robertson AHF, Parlak O, Ünlügenç UC (eds) *Geological development of Anatolia and the Easternmost Mediterranean Region*, vol 372. Geological Society, London, pp 495–529. <https://doi.org/10.1144/sp372.14>
- Duman TY, Emre Ö, Özalp S, Elmacı H, Olgun Ş (2012) 1:250,000 Ölçekli Türkiye Diri Fay Haritası Serisi, Elazığ (NJ 37–7) Paftası, Seri No: 45. Maden Tetkik ve Arama Genel Müdürlüğü, Ankara
- Duman TY, Emre Ö, Özalp S, Çan T, Olgun Ş, Elmacı H, Şaroğlu F (2017) Türkiye ve Yakın Çevresindeki Diri Faylar ve Özellikleri. In: Duman TY (eds) *Türkiye Sismotektonik Haritası Açıklama Kitabı*. Maden Tetkik ve Arama Genel Müdürlüğü Özel Yayınlar Serisi-34, Ankara-Türkiye, 12 s
- Emre Ö, Duman TY, Özalp S, Elmacı H, Olgun Ş, Şaroğlu F (2013) Açıklamalı Türkiye Diri Fay Haritası. Ölçek 1:1.250.000, Maden Tetkik ve Arama Genel Müdürlüğü, Özel Yayın Serisi-30, Ankara-Türkiye.
- Ergin K, Güçlü U, Uz Z (1967) A catalog of earthquake for Turkey and surrounding area (11 A.D. to 1964 A.D.). İTÜ Faculty of Mining Engineering, İstanbul
- ESA (European Space Agency) (2020). <https://scihub.copernicus.eu/dhus/#/home>. Accessed 14 June 2020
- Eyidoğan H, Güçlü U, Utku Z, Değirmenci E (1991) Türkiye Büyük Depremleri Makro-Sismik Rehberi (1900–1988). İTÜ Maden Fakültesi, İstanbul
- Gökçeoğlu C, Şahmaran M, Unutmaz B, Aldemir A, Koçkar MK, Sandıkkaya A, İçen A (2020) 24 Ocak 2020 Elazığ Sivrice Depremi (Mw= 6.8) Ön İnceleme Raporu. Hacettepe Üniversitesi Mühendislik Fakültesi İnşaat Mühendisliği Bölümü, Ankara, p 44
- Goldstein RM, Werner CL (1998) Radar interferogram filtering for geophysical applications. *Geophys Res Lett* 25(21):4035–4038
- Güneyli H (2002) Doğu Anadolu Fay Sistemi, Palu-Hazar Gölü Segmentinin Neotektoniği ve Paleosismolojisi, Doktora Tezi, Çukurova Üniversitesi, Fen Bilimleri Enstitüsü
- Gürsoy H, İnan S, Tatar O, Ünlügenç UC, Demirkol C (1998) Surface deformation, liquefaction-induced features and tectonic setting of 27 June 1998 Adana-Ceyhan earthquake. In: 3rd International Turkish Geology Symposium, Abstracts, METU, 31 August–4 September 1998, Ankara, p 323
- Helz RL (2005) Monitoring ground deformation from space. US Department of the Interior, Washington
- Hempton MR (1985) Structure and deformation history of Bitlis suture near lake Hazar, southeastern Turkey. *Geol Soc Am Bull* 96:233–243
- Hempton MR, Dunne L (1984) Sedimentation in pull-apart basins: active examples in Eastern Turkey. *J Geol* 92:513–530
- Herece E (2008) Doğu Anadolu Fayı (DAF) Atlası. MTA Genel Müdürlüğü, Özel Yayın Serisi, No: 13, Ankara, 359 s

- Herece E, Akay E (1992) Karlıova-Çelikhan arasında Doğu Anadolu Fayı. In: Proceeding of the 9th Petroleum Congress of Turkey. 17–21 February 1992, Ankara, Turkey, pp 361–372
- İTÜ' lü Akademisyenlerden Elâzığ ve Malatya Depremine İlişkin Değerlendirme (2020) 11 Şubat 2020. <https://www.haberturk.com/itulu-akademisyenlerden-elazig-depremine-iliskin-saharaporu-2568984>. Accessed 31 Jan 2020
- Jamalreyhani M, Büyükkapınar P, Cesca S, Dahm T, Sudhaus H, Rezapour M, Heimann S (2020) Seismicity related to the eastern sector of Anatolian escape tectonic: the example of the 24 January 2020 Mw 6.77 Elâzığ-Sivrice earthquake. *Solid Earth Discussions*, pp 1–22.
- Kalafat D, Zülfikar C, Vuran E, Kamer Y (2010) 8 Mart 2010 Başyurt-Karakoçan (Elâzığ) Depremi. Boğaziçi Üniversitesi, İstanbul, p 65
- Kalafat D, Güneş Y, Kekovalı K, Yılmaz M (2011) A revised and extended earthquake catalogue for Turkey since 1900 ($M \geq 4.0$). Boğaziçi University, İstanbul, p 640 (in Turkish)
- KANDİLLİ (2020) B.U. Kandilli Rasathanesi ve Deprem Araştırma Enstitüsü. <https://www.koeri.boun.edu.tr/>. Accessed 20 Feb 2020
- Karabacak V, Önder Y, Altunel E, Yalçınır CC, Akyüz HS, Kıyak NG (2011) Doğu Anadolu Fay Zonunun güney batı uzanımının paleoisomolojisi ve ilk kayma hızı. In: Aktif Tektonik Araştırma Grubu Onbeşinci Çalıştayı (ATAG-15), Çukurova Üniversitesi, 19–22 Ekim 2011, Bildiri özetleri Kitabı, 17, Karataş-Adana.
- Khalifa A, Çakır Z, Owen L, Kaya Ş (2018) Morphotectonic analysis of the East Anatolian Fault, Turkey. *Turk J Earth Sci* 27:110–126
- Koçyiğit A, Rojaj B, Cihan M, Özacar A (2001b) The June 6, 2000, Orta (Çankırı, Turkey) Earthquake: Sourced from a New Antithetic Sinistral Strike-slip Structure of the North Anatolian Fault System, the Dodurga Fault Zone. *Turk J Earth Sci* 10(2001):69–82
- Koçyiğit A, Yılmaz A, Adamia S, Kuloshvili S (2001) Neotectonics of East Anatolian Plateau (Turkey) and Lesser Caucasus: implication for transition from thrusting to strike-slip faulting. *Geodin Acta* 14:177–195
- Köküm M, Özçelik F (2020) Tarihsel Depremlerin Yeniden Değerlendirilmesine Örnek Bir Çalışma: 1789 Palu (Elâzığ) Depremi, Doğu Anadolu, Türkiye. *Maden Tetkik ve Arama Dergisi* 161:1–10
- Kürçer A, Elmacı H, Yıldırım N, Özalp S (2020) 24 Ocak 2020 Sivrice (Elâzığ) Depremi (Mw=6,8) Saha Gözlemleri ve Değerlendirme Raporu. MTA Jeoloji Etütleri Dairesi, New York, p 41
- McKenzie D (1978) Some remarks on the development of sedimentary basins. *Earth Planet Sci Lett* 40(1):25–32
- McClusky S, Balassanian S, Barka A, Demir C, Ergintav S, Georgiev I, Gürkan O, Hamburger M, Hurst K, Kahle H, Kastens K, Kekelidze G, King R, Kotzev V, Lenk O, Mahmoud S, Mishin A, Nadariya M, Ouzounis A, Paradissis D, Peter Y, Prilepin M, Reilinger R, Şanlı İ, Seeger H, Tealeb A, Toksöz MN, Veis G (2000) Global positioning system constraints on plate kinematics and dynamics in the eastern mediterranean and Caucasus. *J Geophys Res* 105:5695–5719
- Melgar D, Ganas A, Taymaz T, Valkaniotis S, Crowell BW, Kapetanidis V, Öcalan T (2020) Rupture kinematics of 2020 January 24 Mw 6.7 Doğanyol-Sivrice, Turkey earthquake on the East Anatolian Fault Zone imaged by space geodesy. *Geophys J Int* 223(2):862–874
- Nalbant SS, McCloskey J, Steacy S, Barka AA (2002) Stress accumulation and increased seismic risk in eastern Turkey. *Earth Planet Sci Lett* 195:291–298
- Örgülü G, Aktar M, Türkelli N, Sandvol E, Barazangi M (2003) Contribution to the seismotectonics of eastern Turkey from moderate and small size events. *Geophys Res Lett*. <https://doi.org/10.1029/2003GL018258>
- Özkaymak Ç, Sözbilir H, Bozkurt E, Dirik K, Topal T, Alan H, Çağlan D (2011) Seismic geomorphology of October 23, 2011 Tabanlı-Van earthquake and its relation to active tectonics of East Anatolia. *Jeoloji Mühendisliği Dergisi* 35(2):175–200
- Özener H, Arpat E, Ergintav S, Doğru A, Çakmak R, Turgut B, Doğan U (2010) Kinematics of the eastern part of the North Anatolian Fault Zone. *J Geodyn* 49:141–150
- Pousse-Beltran L, Nissen E, Bergman EA, Cambaz MD, Gaudreau É, Karasözen E, Tan F (2020) The 2020 Mw 6.8 Elâzığ (Turkey) Earthquake Reveals Rupture Behavior of the East Anatolian Fault. *Geophys Res Lett* 47(13):2020088136
- Reilinger R, McClusky S, Vernant P, Lawrence S, Ergintav S, Cakmak R, Özener H, Kadirov F, Guliev I, Stepanyan R, Nadariya M, Hahubia G, Mahmoud S, Sakr K, ArRajehi A, Paradissis D, Al-Aydrus A, Prilepin M, Guseva T, Evren E, Dmitrotsa A, Filikov SV, Gomez F, Al-Ghazzi R, Karam G (2006) GPS constraints on continental deformation in the Africa-Arabia-Eurasia continental collision zone and implications for the dynamics of plate interactions. *J Geophys Res* 111:B05411. <https://doi.org/10.1029/2005JB004051>
- Şaroğlu F, Yılmaz Y (1987) Doğu Anadolu'da Neotektonik dönemdeki jeolojik evrim ve havza modelleri. *MTA Dergisi* 107:73–92
- Sarychikhina O, Glowacka E (2015) Spatio-temporal evolution of aseismic ground deformation in the Mexicali Valley (Baja California, Mexico) from 1993 to 2010, using differential SAR interferometry. *Proc Int Assoc Hydrol Sci* 372:335
- Şengör AMC, Yılmaz Y (1981) Tethyan evolution of Turkey: a plate tectonic approach. *Tectonophysics* 75:181–241
- Şengör AMC, Görür N, Şaroğlu F (1985) Strike-slip faulting and related basin formation in zones of tectonic escape: Turkey as a case study. In: Biddle KT, Christie-Blick N (eds) Strike-slip faulting and basin formation, vol 37. Society of Economic Paleontologists and Mineralogists, London, pp 227–264
- Tan O, Tapırdamaz MC, ve Yörük A (2008) The earthquakes catalogues for Turkey. *Turk J Earth Sci* 17:405–418
- Tan O, Pabuççu Z, Tapırdamaz C, İnan S, Ergintav S, Eyidoğan H, Aksoy E, Kuluöztürk F (2011) Aftershock study and seismotectonic implications of the 8 March 2010 Kovancılar (Elâzığ, Turkey) earthquake (MW = 6.1). *Geophys Res Lett*. <https://doi.org/10.1029/2011GL047702>
- Taymaz T, Eyidoğan H, Jackson J (1991) Source parameters of large earthquakes in the East Anatolian Fault Zone (Turkey). *Geophys J Int* 106(3):537–550
- Taymaz T, Yılmaz Y, Dilek Y (2007) The geodynamics of the Aegean and Anatolia: introduction. *Geol Soc Lond Spec Publ* 291:1–16
- Toksöz MN, Arpat E, Şaroğlu F (1977) East Anatolian earthquake of 24 November 1976. *Nature* 270(5636):423–425
- Torres R, Snoeij P, Geudtner D, Bibby D, Davidson M, Attema E, Traver IN (2012) GMES Sentinel-1 mission. *Remote Sens Environ* 120:9–24
- Türkelli N, Sandvol E, Zor E, Gök R, Bekler T, Al-Lazki A, Karabulut H, Kuleli S, Eken T, Gürbüz C, Bayraktutan S, Şeber D, Barazangi M (2003) Seismogenic zones in eastern Turkey. *Geophys Res Lett* 30(24).
- Westaway R (2003) Kinematics of the Middle East and Eastern Mediterranean updated. *Turk J Earth Sci* 12:5–46
- Westaway R, Arger J (1996) The Gölbaşı basin, southeastern Turkey: a complex discontinuity in a major strike-slip fault zone. *J Geol Soc (Lond)* 153:729–743
- Westaway R, Arger J (2001) Kinematics of the Malatya-Ovacık fault zone. *Geodin Acta* 14:103–132
- Yagüe-Martínez N, Prats-Iraola P, Gonzalez FR, Brcic R, Shau R, Geudtner D, Bamler R (2016) Interferometric processing of Sentinel-1 TOPS data. *IEEE Trans Geosci Remote Sens* 54(4):2220–2234

- Yılmaz Y (1993) New evidence and model on the evolution of the southeast Anatolian Orogen. *Geol Soc Am Bull* 105:251–271
- Yılmaz Y, Şaroğlu F, ve Güner Y (1987) Initiation of the neomagmatism in East Anatolia. *Tectonophysics* 134:177–199
- Yönlü Ö, Altunel E, Karabacak V (2017) Geological and geomorphological evidence for the southwestern extension of the East Anatolian Fault Zone, Turkey. *Earth Planet Sci Lett* 469:1–14

Affiliations

Orhan Tatar¹ · Hasan Sözbilir^{2,3} · Fikret Koçbulut¹ · Erdin Bozkurt^{4,5} · Ercan Aksoy⁶ · Semih Eski³ · Bülent Özmen⁷ · Hüseyin Alan^{8,9} · Yüksel Metin¹⁰

✉ Orhan Tatar
orhantatar@cumhuriyet.edu.tr

¹ Mühendislik Fakültesi, Sivas Cumhuriyet Üniversitesi, Jeoloji Mühendisliği Bölümü, Kampüs, 58140 Sivas, Turkey

² Dokuz Eylül Üniversitesi, Deprem Araştırma ve Uygulama Merkezi, Doğu Caddesi No: 207/A, Tınaztepe Yerleşkesi, Buca, 35390 İzmir, Turkey

³ Mühendislik Fakültesi, Jeoloji Mühendisliği Bölümü, Dokuz Eylül Üniversitesi, Doğu Caddesi No: 207/A, Tınaztepe Yerleşkesi, Buca, 35390 İzmir, Turkey

⁴ Jeoloji Mühendisliği Bölümü, Orta Doğu Teknik Üniversitesi, Dumlupınar Bulvarı No: 1, 06800 Ankara, Turkey

⁵ Center for Global Tectonics and State Key Laboratory of Geological Processes and Mineral Resources, University of Geosciences, 388 Lumo Road, Hongshan District, Wuhan 430074, Hubei, China

⁶ Jeoloji Mühendisliği Bölümü, Mühendislik Fakültesi, Fırat Üniversitesi, 23119 Elâzığ, Turkey

⁷ Mühendislik Fakültesi, Gazi Üniversitesi Deprem Mühendisliği Uygulama ve Araştırma Merkezi, Eti Mahallesi, Yükseliş Sokak No: 5, 06570 Maltepe, Ankara, Turkey

⁸ T.C. Çevre ve Şehircilik Bakanlığı, Mustafa Kemal Mahallesi, Eskişehir Devlet Yolu (Dumlupınar Bulvarı) 9. km, No: 278, 06650 Çankaya, Ankara, Turkey

⁹ TMMOB Jeoloji Mühendisleri Odası, Hatay Sokak No: 21, 06420 Ankara, Turkey

¹⁰ Maden Tetkik ve Arama Genel Müdürlüğü, Çukurambar Mahallesi, Dumlupınar Bulvarı No: 33/A, 06800 Çankaya, Ankara, Turkey